Joint Defra/EA Flood and Coastal Erosion Risk Management R&D Programme

FD2120: Analysis of historical data sets to look for impacts of land use management change on flood generation

A4. Technical appendix: Analyses of catchment data sets

R&D Project Record FD2120/PR

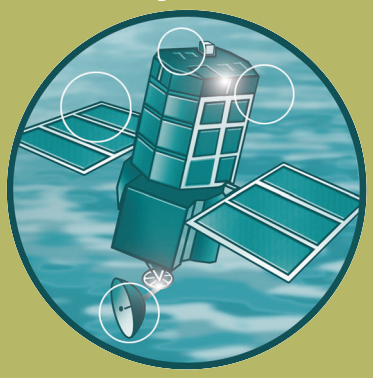

Environment Agency

defra
Department for Environment Food and Rural Affairs

A4 TECHNICAL APPENDIX: ANALYSES OF CATCHMENT DATA SETS

Renata Romanowicz, Keith Beven and Peter Young
Environmental Science, Lancaster University, Lancaster LA1 4YQ.

A4.1 Bain Catchment

A4.1.1 Catchment data

The Bain catchment (197 km^2) is rural, mostly clay with chalk and sandstone in the headwaters. Flow data from the gauging station at Fulsby start on the 06/11/1979 and end on the 29/02/2004. The flow data quality is poor, with many missing values replaced by zeros, or obvious measurement errors.

Rainfall data from the rain gauge at Fulsby start on the 01/01/1987 00:00 and end on the 27/03/2003. Figure A4.1 presents the rainfall-flow data for Bain on a common time period 1987-2003.

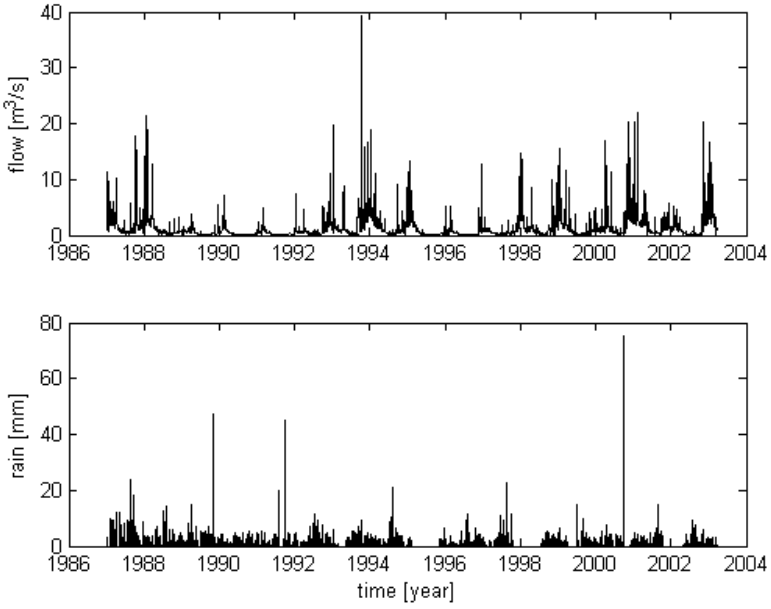

Figure A4.1. Flow and rainfall hourly data for Bain

A4.1.2 DHR analysis

DHR analysis was performed on the logarithms of monthly averaged flows and monthly sums of daily rainfall in order to decompose the time series into trend and periodic components.

The resulting trend for the logarithm of monthly flow is shown on the upper panel of Figure A4.2. The lower panel shows the trend obtained for the monthly sums of rainfall. There are also shown 0.95 confidence bands for the trends (red dotted lines) and observations are marked by black dots.

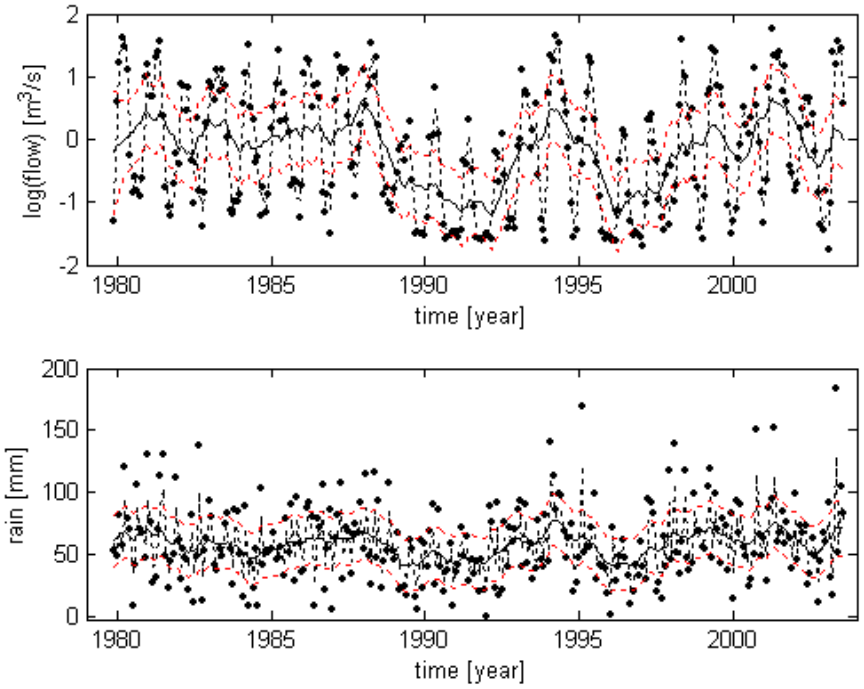

Figure A4.2 Comparison of trend of logarithm of monthly flow (upper panel) and monthly rainfall (lower panel); red dotted line denote 0.95 confidence bounds for the trend, black dots denote the observations

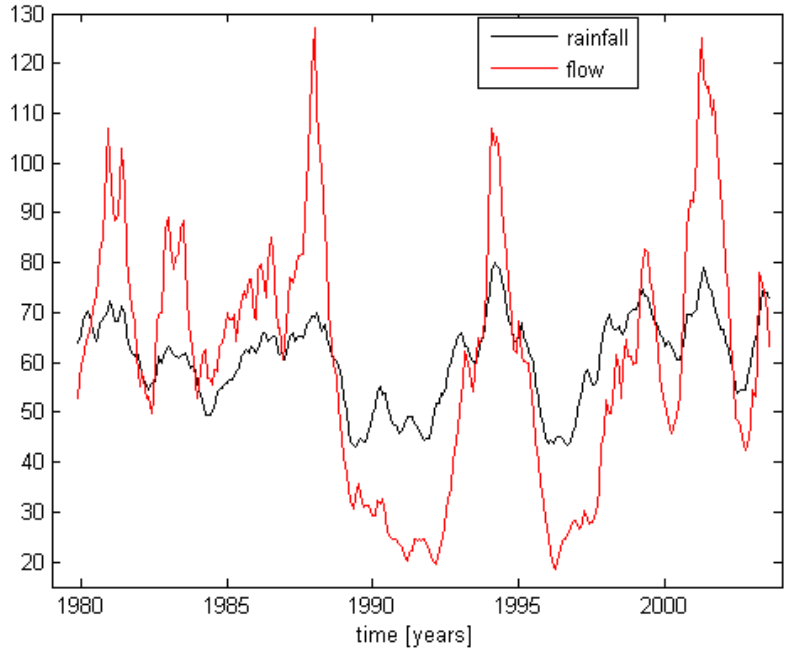

Figure A4.3 Nonstationary trends in monthly rainfall and flows in the Bain catchment scaled to equal total volumes

In order to obtain a quantitative comparison, Figure A4.3 presents the nonstationary monthly trends for the Bain catchment, based on the normalised trends of monthly flows and rainfall for the years 1979-2003. The discharges were scaled to an equivalent rainfall depth for the purpose of comparison of the temporal changes. Monthly flow trend shows larger variability in the period 1988-2003 than in the period 1979-1987.

Normal statistical tests for rainfall and flow trends were both negative.

A4.1.3 DBM analysis.

Following the description of the approach given in Technical Appendix 3, the first stage of the analysis was based on selected periods from the full event length data. The length of the periods was chosen to cover the full high-flow season from Autumn to Spring, with exceptions were data were missing. We analysed 25 periods over the years 1979-2003, from 1000 to 6500 hours long. The identified TF model has the form [2 2 0 0] for most of the analysed events, with the exception of the last 4 events, where the model [2 2 5 0] was preferable. This indicates some inconsistencies in the data, but we did not have to delay the flows, as in the case of Axe catchment. The list of TF model parameters is given in Table A4.1. The estimated effective rainfall nonlinearity has an exponential shape, as for the Axe catchment. The parameters of second order models a_1, a_2, b_0, b_1 were estimated together with the effective rainfall parameter γ. The first column of the

table (period) refers to the middle point of the time horizon of each event. The goodness of fit criterion R_T^2 is given in the last column.

Table A4.1 DBM model parameters for the Bain catchment.

period	a_1	a_2	b_0	b_1	γ	R_T^2
1987.62	-1.97	0.97	0.0068	-0.0068	0.0510	0.77
1988.30	-1.97	0.97	0.0126	-0.0125	0.0000	0.79
1989.03	-1.73	0.73	0.0012	0.0001	0.0038	0.18
1989.85	-1.98	0.98	0.0040	-0.0040	0.0036	0.86
1990.47	-1.98	0.98	0.0062	-0.0061	0.0000	0.80
1991.21	-1.98	0.98	0.0077	-0.0077	0.0000	0.00
1991.67	-1.97	0.97	0.0092	-0.0091	0.0000	0.78
1992.36	-1.95	0.95	0.0127	-0.0126	0.3940	0.69
1992.87	-1.92	0.93	0.0212	-0.0208	0.0000	0.85
1993.27	-1.91	0.91	0.0128	-0.0125	0.3089	0.68
1994.13	-1.95	0.95	0.0207	-0.0207	0.2396	0.78
1994.64	-1.93	0.93	0.0079	-0.0077	0.2999	0.88
1994.92	-1.95	0.95	0.0244	-0.0243	0.2637	0.87
1995.47	-1.98	0.98	0.0041	-0.0041	0.6598	0.64
1996.06	-1.89	0.89	0.0210	-0.0207	0.0000	0.82
1996.51	-1.98	0.98	0.0095	-0.0095	0.3830	0.84
1996.98	-1.91	0.91	0.0311	-0.0304	0.5466	0.90
1997.74	-1.96	0.96	0.0122	-0.0121	0.0154	0.84
1998.04	-1.98	0.98	0.0056	-0.0055	0.7394	0.77
1999.17	-1.47	0.48	0.0030	0.0006	0.0184	0.80
2000.17	-1.36	0.36	0.0026	-0.0001	0.0000	0.74
2000.86	-1.97	0.97	0.0051	-0.0051	0.0180	0.13
2001.68	-1.97	0.97	0.0094	-0.0093	0.0172	0.76
2002.77	-1.98	0.98	0.0066	-0.0066	0.0302	0.83
2003.26	-1.97	0.97	0.0133	-0.0133	0.2658	0.87

The nonlinear gains defined as $g_k = s_0 \cdot (1 - \exp(\gamma \cdot y_k)$, obtained for all the feasible models shown in Table A4.1 are illustrated in Figures A4.4a, b. Some of the gains have straight lines, indicating that power model for the parameterisation of nonlinear rainfall-flow relationship might be better. However we did not want to introduce different parameterisation function as we would not be able to compare the events.

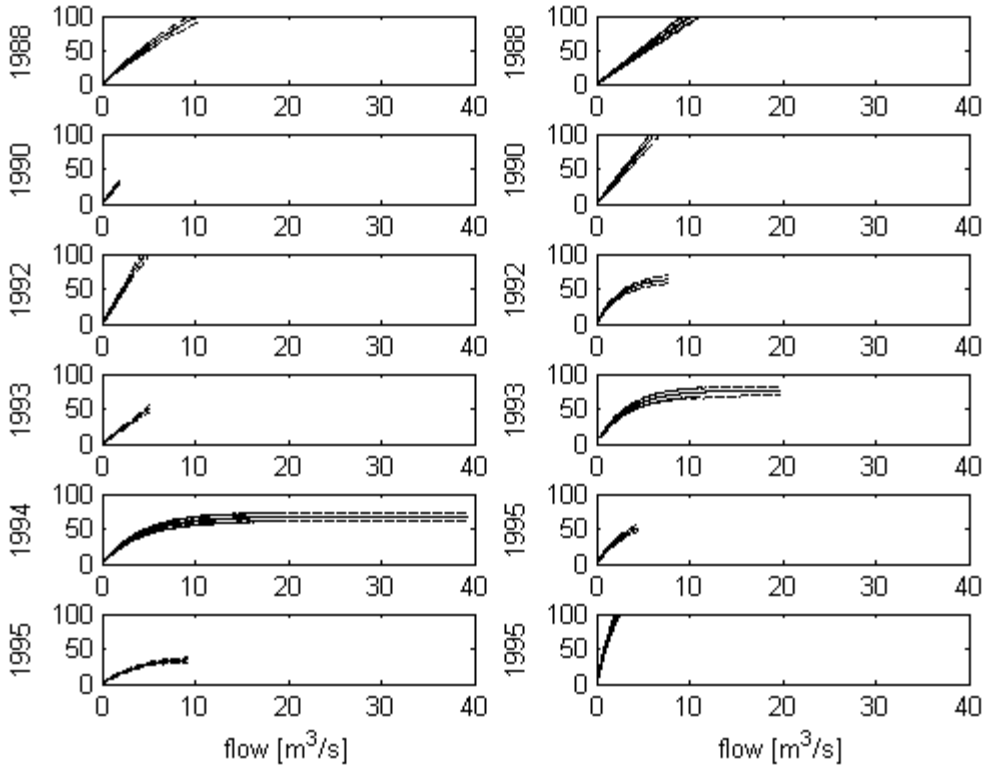

Figure A4.4a Nonlinear gains for the years 1988-1995 with 0.95 confidence bounds

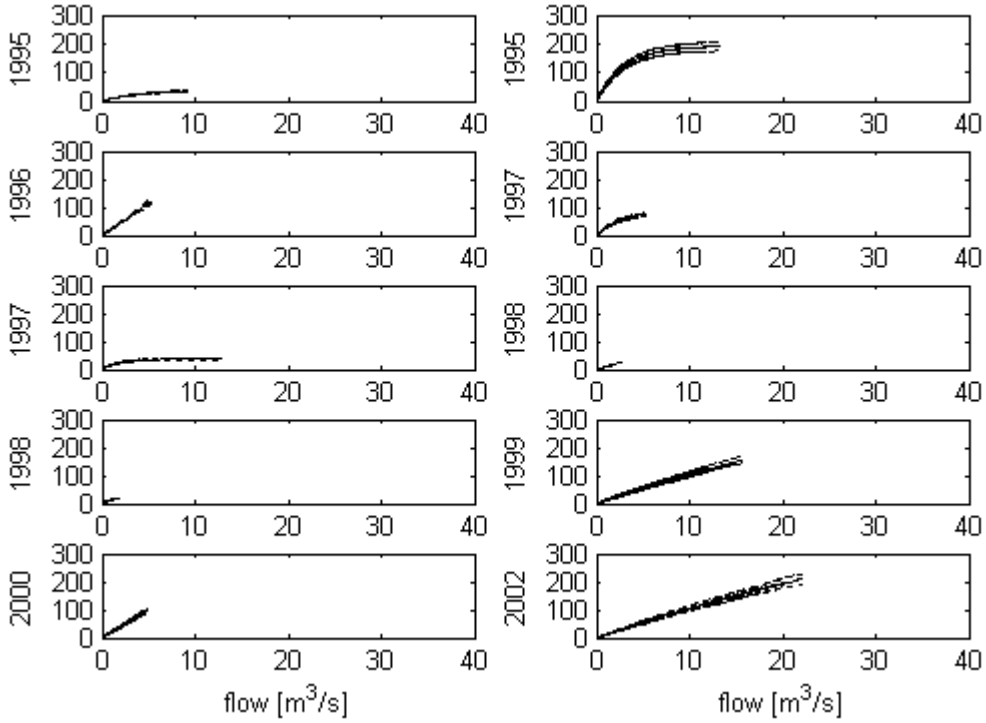

Figure A4.4b Nonlinear gains for the years 1995-2002 with 0.95 confidence bounds

A4.1.4 Analysis of DBM Results for Bain

The MC analysis was performed on the model parameters derived from the DBM model after the decomposition into fast and slow response (see Technical Appendix 3). The results of the MC analysis for the proportions are shown in Figure A4.5, upper panel showing the slow and lower panel showing the fast model component.

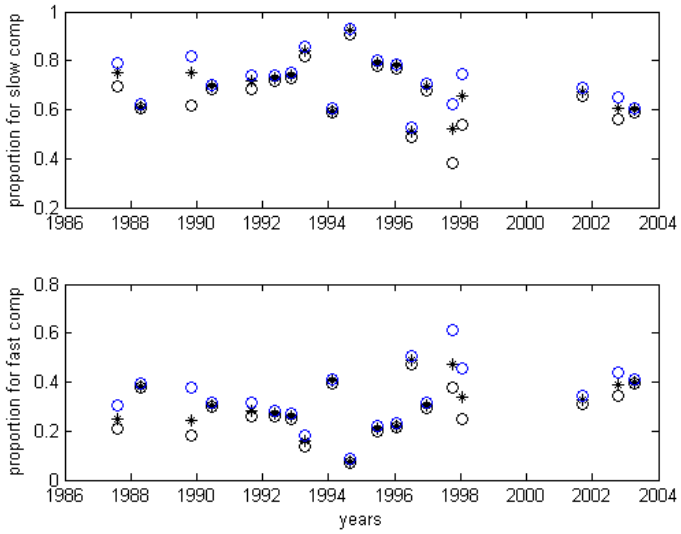

Figure A4.5. Proportions (black dots) with 0.95 confidence bounds (black and blue circles) for Bain catchment

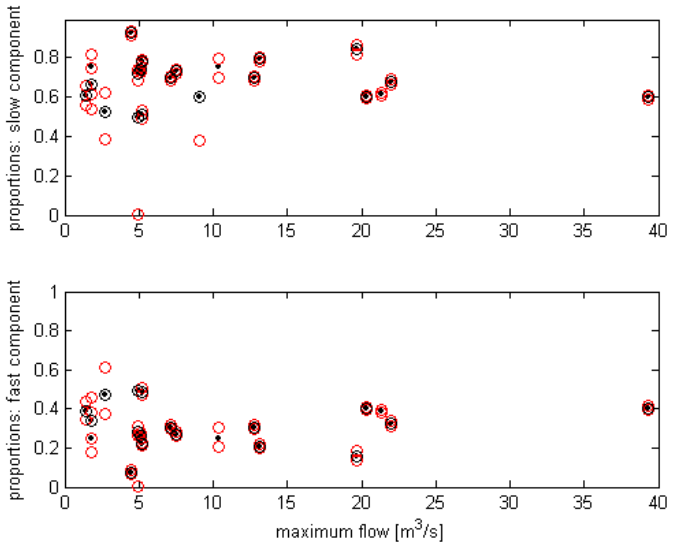

Figure A4.6. Proportions (black dots) with 0.95 confidence bounds (red circles) against maximum flow for Bain catchment

Figure A4.6 presents the proportions against maximum flow for each of the events. Black circles mark events which happened after 1994.

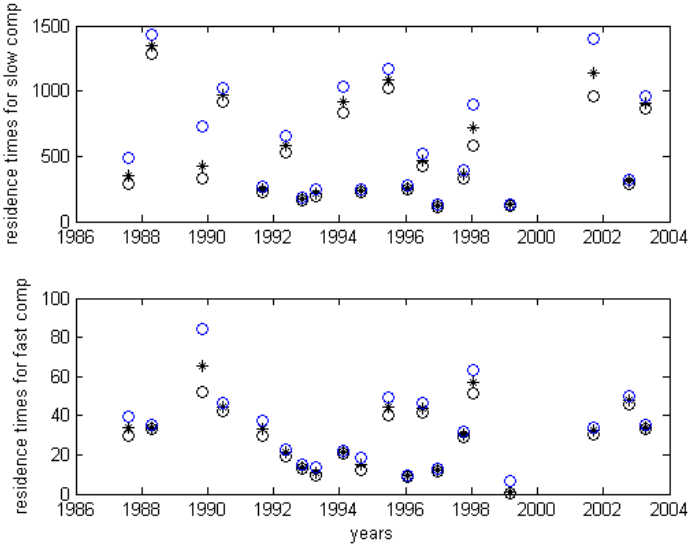

Figure A4.7. Residence times (hours) (black dots) with 0.95 confidence bounds (black and blue circles) for Bain catchment

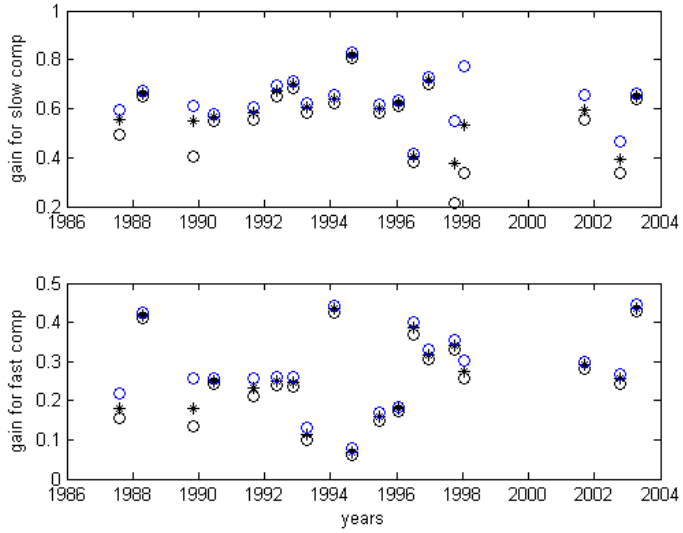

Figure A4.8. Gains (black dots) with 0.95 confidence bounds (black and blue circles) for Bain catchment

The residence times against time are presented in Figure A4.7 and Figure A4.8 shows the gains together with their upper and lower bounds obtained from MC analysis.

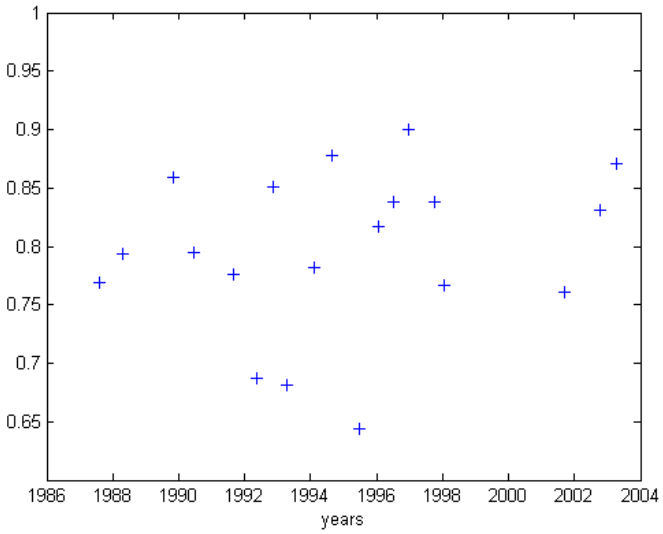

Figure A4.9. Goodness of fit criterion (rt2) for each DBM model

The results of the DBM model analysis for Bain show reasonable fits to the data (Figure A4.9) but no evidence of any trends or relationship between the derived variables and maximum flows.

A4.2 Blyth Catchment

A4.2.1 Catchment data

The available flow data for the Blythe Catchment (268 km^2) start on the 29/03/1983 at 18:00 and end on the 03/02/2004 at 11:45. Two sets of tipping bucket rainfall data were available. Rainfall data from the gauge at Darras Hall start on the 01/01/1986 00:00 and end on the10/08/2003 00:00. The other set of rainfall data consists of two concatenated records from Wallington Logger and Wallington Hall, starting on the 01/01/1983 and finishing on the 10/08/2003.

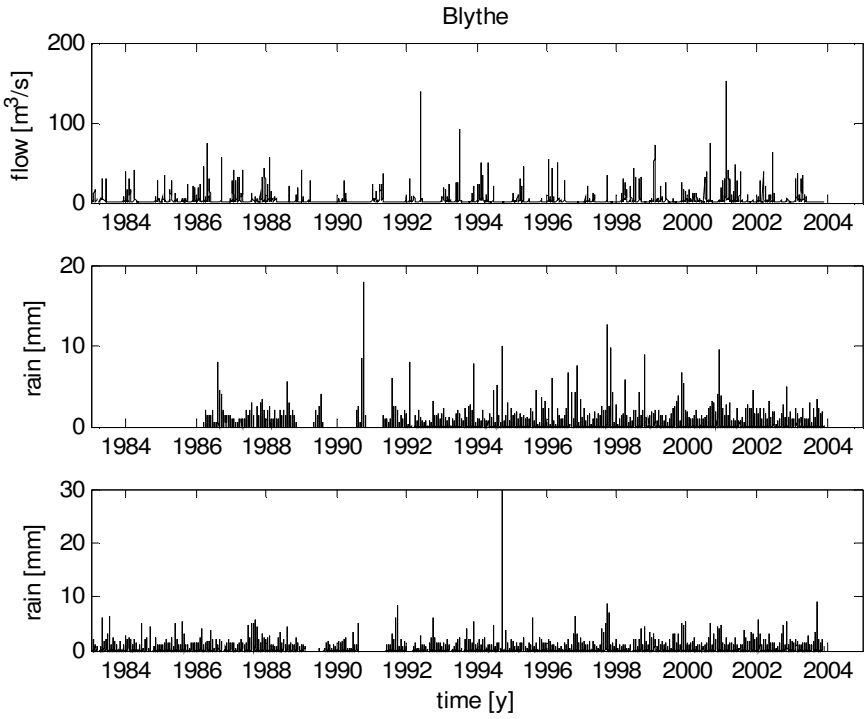

Figure A4.10 Flow and rainfall data for Blyth

Figure A4.10 presents the rainfall-flow data for Blyth on a common time period 1983-2003. The rainfall data from both gauging stations were combined together based on the longer record. However, some periods of missing data still remained in 1989 and 1990.

A4.2.2 DHR analysis

Figures A4.11 illustrates the application of the DHR method to logarithms of monthly flow and sums of monthly rainfall. Monthly records are used in this stage of the analysis

to filter out the high variability of the daily records, particularly in the rainfalls. Using the DHR methods we are looking for long term trends in the data and modelled frequency components of the data, not changes in the short term catchment dynamics. Figure A4.11 shows the identified trend in the log discharges together with 0.95 confidence bounds shown in red. Figure A4.12 shows the normalised trends after normalising the discharge trends as before. Neither trend was significant based on a normal significance test.

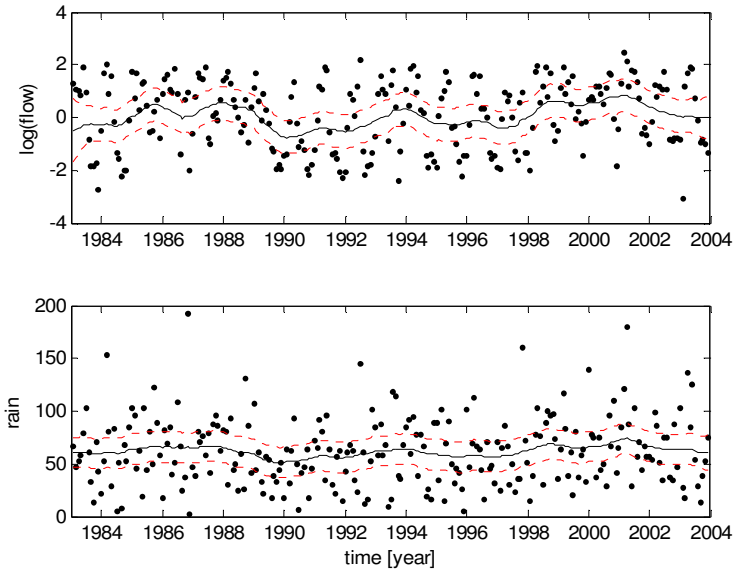

Figure A4.11. Blyth catchment. Comparison of trend of logarithm of monthly flow (upper panel) and monthly rainfall (lower panel); red dotted line denote 0.95 confidence bounds for the trend, black dots denote the observations.

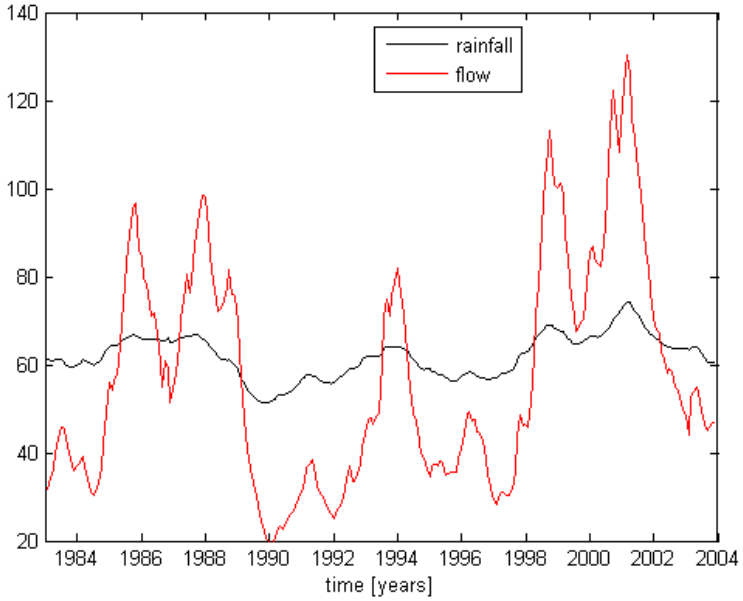

Figure A4.12 Nonstationary trends in monthly rainfall and flows in the Blyth catchment scaled to equal total volumes

A4.2.3 DBM Analysis

Table A4.2 present the results of the DBM modelling of rainfall-runoff dynamics applied to the Blyth catchment for higher flow Autumn-Winter periods of about 6 months long in each year. The identified transfer function model for this catchment was second order with zero delay. The estimated effective rainfall nonlinearity has an exponential shape, similar to the Axe catchment. The parameters of second order models a_1, a_2, b_0, b_1 were estimated together with the effective rainfall parameter γ. The first column of the table (period) refers to the middle point of the time horizon of each event. The goodness of fit criterion R_T^2 is given in the last column. Fit was variable from year to year (also Figure 4.11) with very good fits in some years.

Table A4.2 Parameters of the DBM model for Blyth

Period	a_1	a_2	b_0	b_1	γ	R_T^2
1984.07	-1.73	0.74	0.05	-0.04	0.16	0.66
1985.08	-1.93	0.93	0.02	-0.02	0.08	0.73
1986.11	-1.70	0.70	0.05	-0.05	0.05	0.59
1987.11	-1.79	0.79	0.05	-0.05	0.10	0.60
1988.11	-1.86	0.86	0.03	-0.03	0.13	0.70
1988.95	-1.89	0.89	0.03	-0.03	0.03	0.92
1990.12	-1.83	0.83	0.03	-0.03	0.14	0.77
1990.29	-1.85	0.85	0.03	-0.03	0.15	0.82
1992.24	-1.84	0.84	0.06	-0.06	0.01	0.92
1992.98	-1.89	0.89	0.03	-0.03	0.15	0.83
1994.11	-1.79	0.79	0.06	-0.05	0.10	0.67
1995.11	-1.82	0.83	0.04	-0.04	0.12	0.77
1996.11	-1.91	0.91	0.03	-0.03	0.04	0.79
1997.11	-1.93	0.93	0.02	-0.02	0.03	0.86
1997.99	-1.93	0.93	0.03	-0.03	0.12	0.87
1998.87	-1.88	0.88	0.04	-0.04	0.08	0.92
2000.12	-1.72	0.72	0.05	-0.05	0.07	0.81
2000.99	-1.81	0.81	0.06	-0.06	0.02	0.83
2002.12	-1.90	0.90	0.04	-0.04	0.11	0.73
2002.99	-1.91	0.91	0.03	-0.03	0.05	0.82

The effective rainfall nonlinearity for the years 1983-1992 is shown in Figure 4.13a, and for the years 1993-2003 in Figure 4.13b.

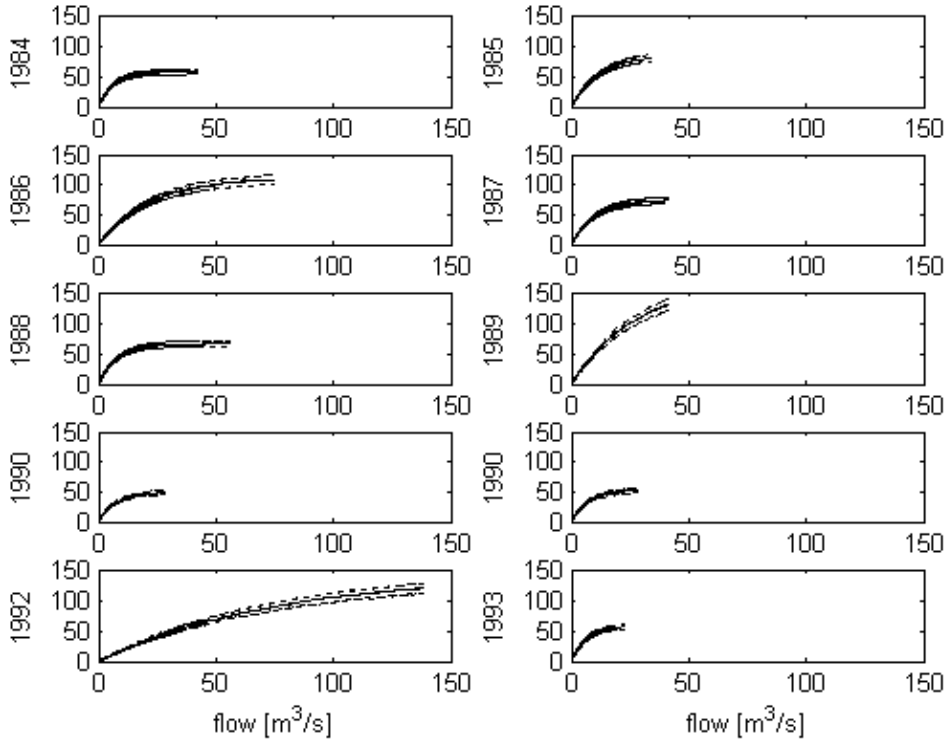

Figure A4.13 a Nonlinear gains for the years 1983-1993 with 0.95 confidence bounds

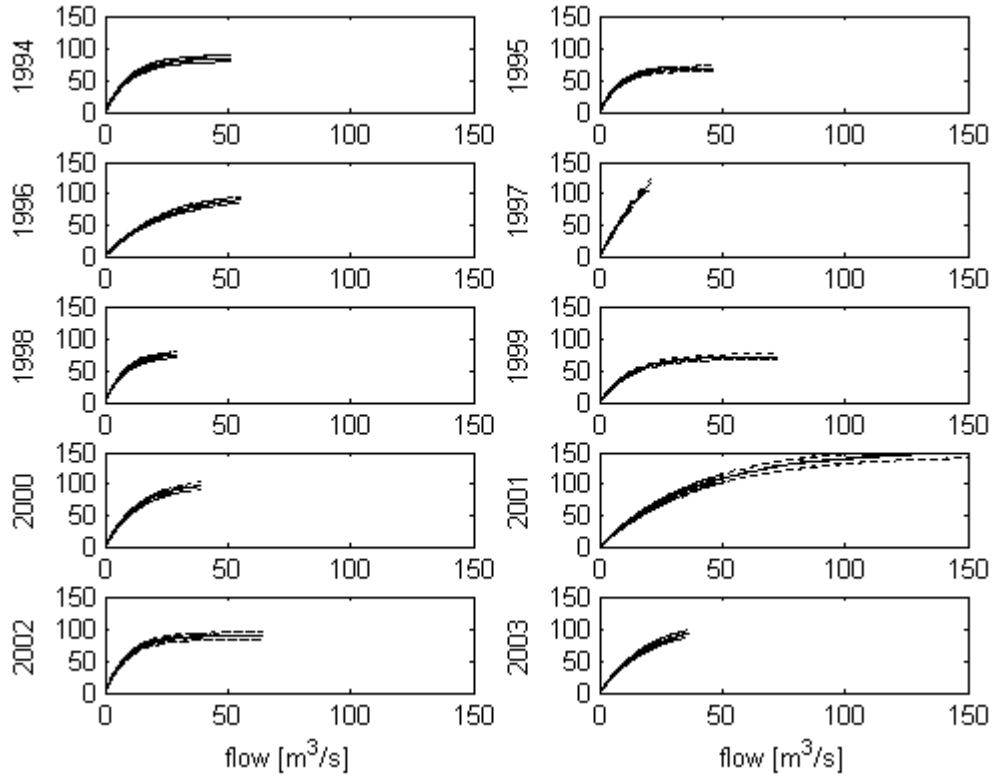

Figure A4.13b Nonlinear gains for the years 1984-2003 with 0.95 confidence bounds

2.1 Analysis of DBM Results for Blyth

The parameters of the models were found to vary significantly from year to year relative to the uncertainty in the values identified for each year. Results are shown for proportions between fast and slow flow components (Figures A4.14), residence times (Figures A4.16) and gains (Figures A4.18). Figures A4.15, A4.17 and A4.19 show respectively, the proportions between fast and slow components, residence times and gains as a function of maximum flow. The goodness of fit values (R_T^2) of each DBM model also varied from year to year and are shown in Figure A4.20.

These results show increased variability at the end of the period of analysis, particularly in the slow component residence time following the dry year of 1995. Any trends in any of these characteristics of the dynamic response, however, are obscured by the year to year variability, with the slow component proportion and gain showing a tendency to decrease with the maximum flow in the period, and the fast component proportion and showing a tendency to increase (and residence time to decrease slightly) with the maximum flow.

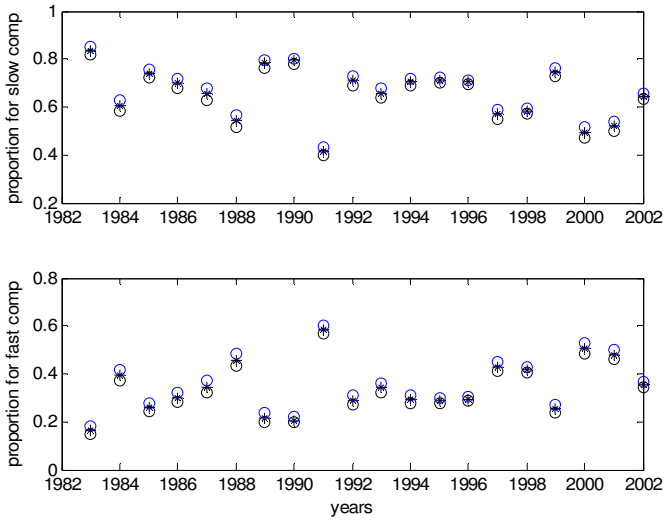

Figure A4.14. Blyth catchment. Proportions of total discharge with 0.95 confidence bounds identified for slow component (upper panel) and fast flow component (lower panel).

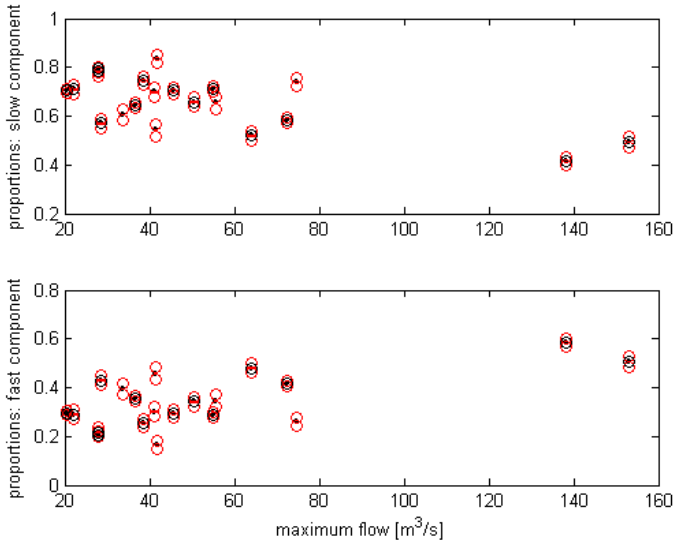

Figure A4.15 Proportions as a function of maximum flow (black dots) with 0.95 confidence bounds (red circles) against maximum flow. Black circles denote events from the years 1991-2003

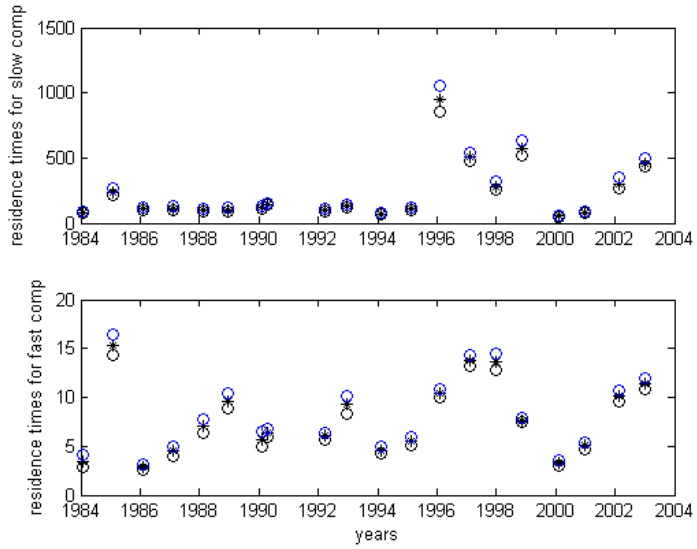

Figure A4.16. Blyth catchment. Identified residence times (hours) with 0.95 confidence bounds for slow component (upper panel) and fast flow component (lower panel).

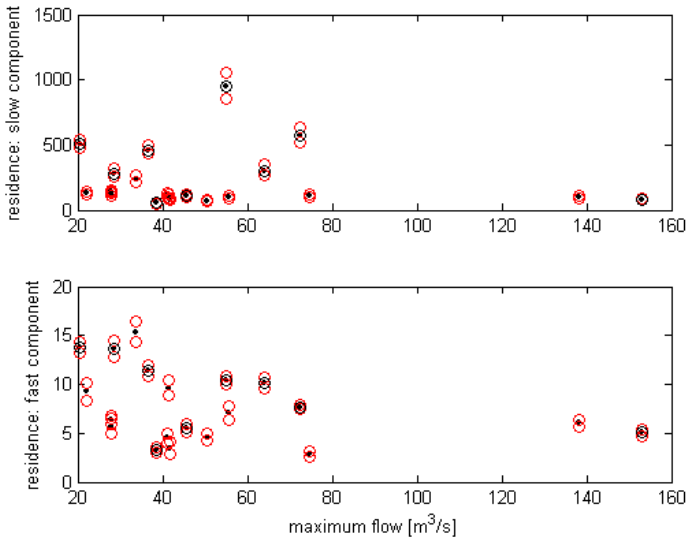

Figure A4.17 Residence times (hours) (black dots) with 0.95 confidence bounds (red circles) against maximum flow, Blyth catchment. Black circles denote events from the years 1991-2003

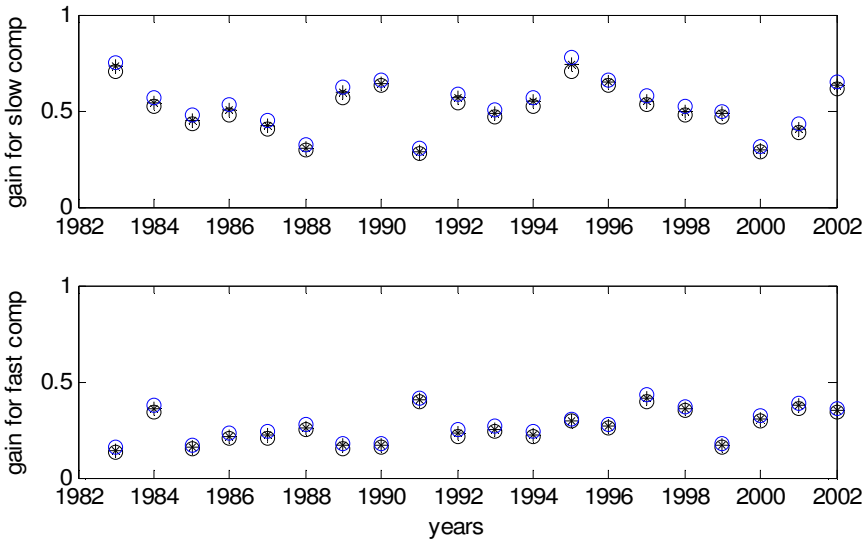

Figure A4.18. Blyth catchment. Identified gains with 0.95 confidence bounds for slow component (upper panel) and fast flow component (lower panel).

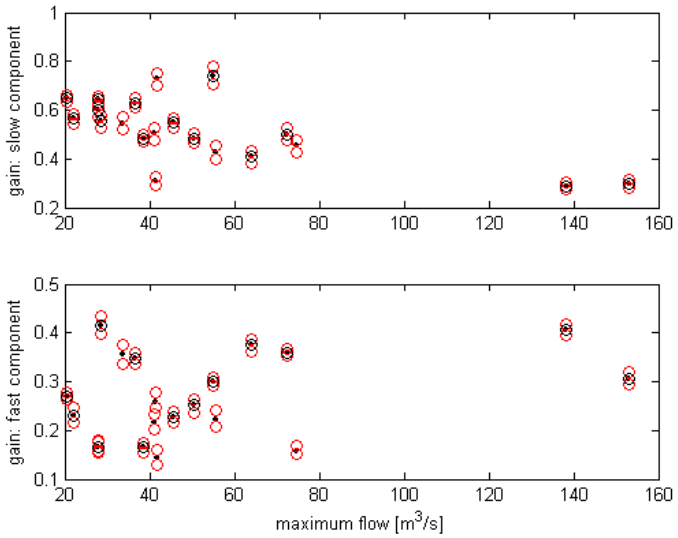

Figure A4.19 Gains (black dots) with 0.95 confidence bounds (red circles) against maximum flow, Blyth catchment. Black circles denote events from the years 1991-2003

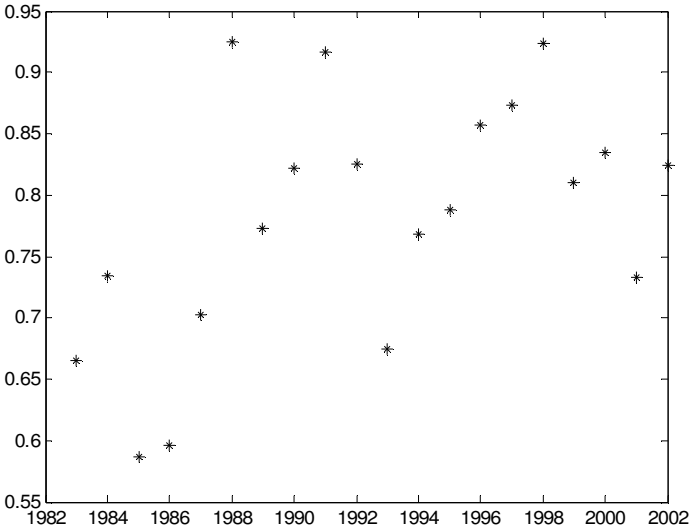

Figure A4.20. Blyth catchment. Goodness of fit R_T^2 values for DBM model for each year.

A4.3 Irthing Catchment

A4.3.1 Catchment data

The flow data for the Irthing Catchment (335 km^2) begin on the 08/01/1975, and end on the 02/03/2004. There are some short periods of missing values which were interpolated using the CAPTAIN toolbox.

There are three rainfall quarterly datasets starting on the 02/03/1992, 31/12/1992 and 04/05/1993 and ending on the 04, 02 and 01/07/2003 respectively.

Hourly rainfall (upper panel) and flow data lower panel) on common period of time are presented in Figure A4.21.

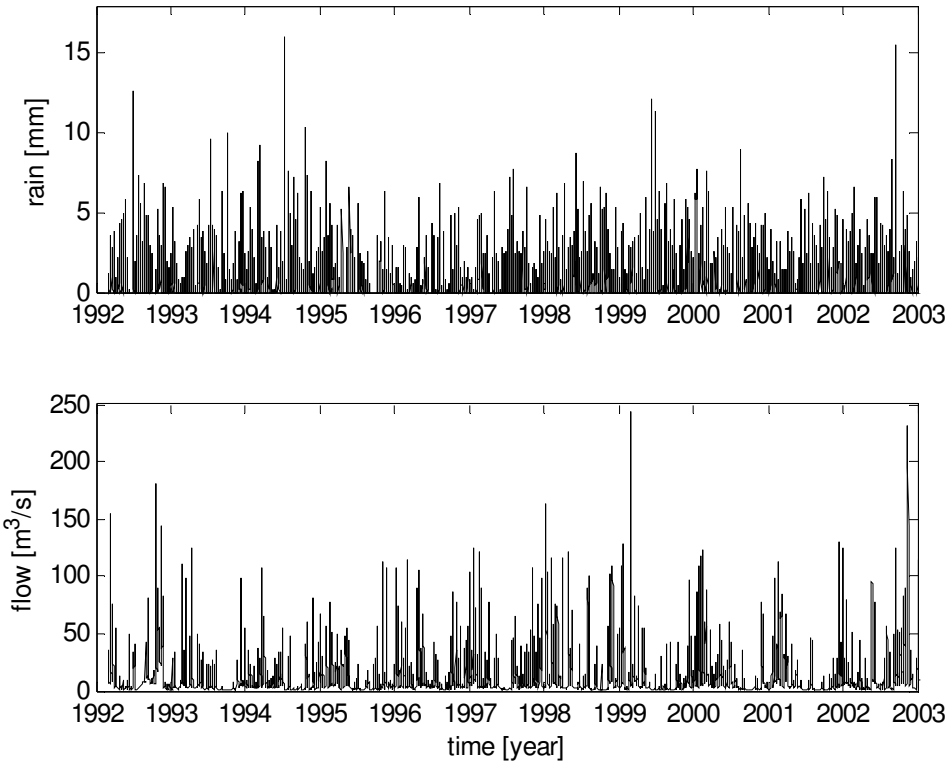

Figure A4.21. Flow and rainfall data for Irthing.

A4.3.2 DHR analysis

Figure A4.22 illustrates the application of the DHR method to logarithms of monthly flow and sums of monthly rainfall for the River Irthing. Monthly records are used in this stage of the analysis to filter out the high variability of the daily records, particularly in the rainfalls. Using the DHR methods we are looking for long term trends in the data and modelled frequency components of the data, not changes in the short term catchment dynamics. Figure A4.22 shows the identified trend in the log discharges together with 0.95 confidence bounds shown in red (upper panel) and trend of monthly rainfall on the lower panel. Figure A4.23 shows the normalised trends after normalising the discharge trends as before. Neither trend was significant based on a normal significance test.

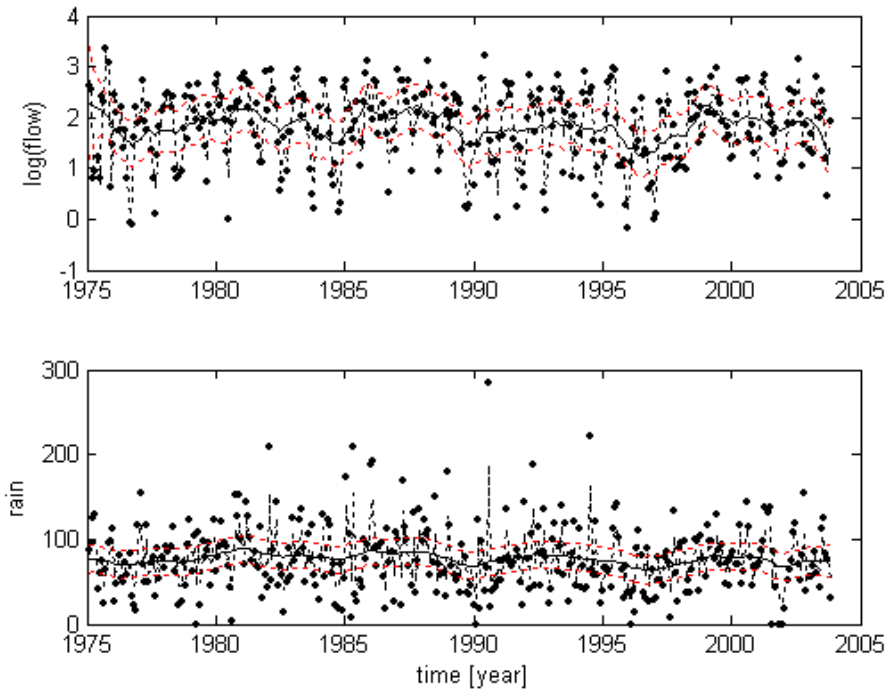

Figure A4.22 Comparison of trend of logarithm of monthly flow (upper panel) and monthly rainfall (lower panel); red dotted line denote 0.95 confidence bounds for the trend, black dots denote the observations.

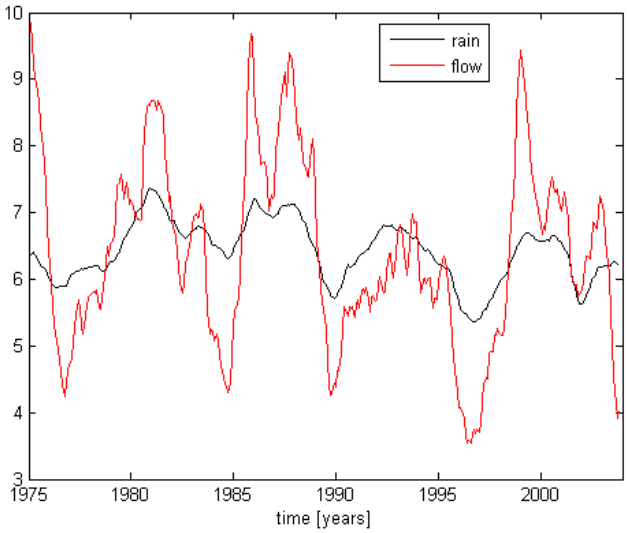

Figure A4.23 Nonstationary trends in monthly rainfall and flows in the Irthing catchment scaled to equal total volumes

A4.3.3 DBM Analysis

Table A4.3 present the results of the DBM modelling of rainfall-runoff dynamics applied to the Irthing catchment for higher flow Autumn-Winter periods of about 6 months long in each year. The identified transfer function model for this catchment was second order with zero delay. The estimated effective rainfall nonlinearity has an exponential shape, similar to the previous catchments. The parameters of second order models a_1, a_2, b_0, b_1 were estimated together with the effective rainfall parameter γ. The first column of the table (period) refers to the middle point of the time horizon of each event. The goodness of fit criterion R_T^2 is given in the last column (see also Figure A4.30).

Table A4.3 Parameters of the DBM model for Irthing

period	a_1	a_2	b_0	b_1	γ	R_T^2
1992.12	-1.61	0.62	0.09	-0.09	0.02	0.77
1992.36	-1.85	0.85	0.04	-0.04	0.01	0.92
1992.61	-1.66	0.67	0.07	-0.06	0.07	0.79
1992.86	-1.80	0.80	0.05	-0.05	0.02	0.55
1993.11	-1.85	0.86	0.05	-0.05	0.07	0.88
1993.36	-1.77	0.77	0.07	-0.07	0.04	0.86
1993.55	-1.93	0.93	0.03	-0.03	0.16	0.68
1993.79	-1.83	0.83	0.06	-0.06	0.04	0.77
1994.10	-1.75	0.76	0.08	-0.08	0.05	0.79
1994.33	-1.93	0.93	0.01	-0.01	0.00	0.49
1994.58	-1.79	0.79	0.08	-0.08	0.02	0.80
1994.84	-1.81	0.81	0.09	-0.09	0.02	0.83
1995.08	-1.78	0.78	0.06	-0.06	0.02	0.78

1995.33	-1.79	0.80	0.06	-0.05	0.02	0.88
1995.57	-1.94	0.94	0.02	-0.02	0.06	0.68
1995.80	-1.81	0.81	0.05	-0.05	0.04	0.73
1996.05	-1.87	0.87	0.03	-0.03	0.02	0.51
1996.32	-1.84	0.84	0.04	-0.04	0.02	0.89
1996.53	-1.91	0.91	0.03	-0.03	0.05	0.83
1996.73	-1.88	0.88	0.05	-0.05	0.06	0.81
1997.01	-1.77	0.77	0.09	-0.09	0.04	0.85
1997.31	-1.80	0.81	0.05	-0.05	0.06	0.90
1997.56	-1.83	0.83	0.04	-0.04	0.03	0.86
1997.80	-1.88	0.88	0.06	-0.06	0.06	0.82
1998.04	-1.80	0.80	0.07	-0.07	0.07	0.82
1998.26	-1.87	0.87	0.05	-0.05	0.07	0.84
1998.52	-1.79	0.79	0.08	-0.08	0.06	0.66
1998.77	-1.86	0.86	0.06	-0.06	0.03	0.75
1998.97	-1.82	0.82	0.04	-0.04	0.01	0.23
1999.21	-1.79	0.80	0.05	-0.05	0.16	0.71
1999.46	-1.70	0.70	0.07	-0.07	0.08	0.79
1999.71	-1.85	0.85	0.06	-0.06	0.03	0.76
1999.95	-1.62	0.62	0.12	-0.11	0.02	0.76
2000.20	-1.73	0.73	0.08	-0.07	0.03	0.86
2000.42	-1.46	0.49	0.03	-0.02	0.01	0.70
2000.67	-1.82	0.82	0.07	-0.07	0.02	0.72
2000.94	-1.91	0.91	0.03	-0.03	0.02	0.76
2001.19	-1.86	0.86	0.05	-0.04	0.13	0.69
2001.43	-1.90	0.90	0.04	-0.04	0.08	0.85
2001.68	-1.74	0.74	0.08	-0.08	0.03	0.68
2001.93	-1.82	0.83	0.13	-0.11	0.07	0.73
2002.17	-1.90	0.90	0.04	-0.04	0.04	0.77
2002.42	-1.83	0.84	0.09	-0.09	0.09	0.77
2002.67	-1.87	0.87	0.07	-0.07	0.04	0.84
2002.91	-1.77	0.78	0.06	-0.05	0.06	0.68
2003.19	-1.90	0.91	0.03	-0.03	0.02	0.84
1992.12	-1.61	0.62	0.09	-0.09	0.02	0.77

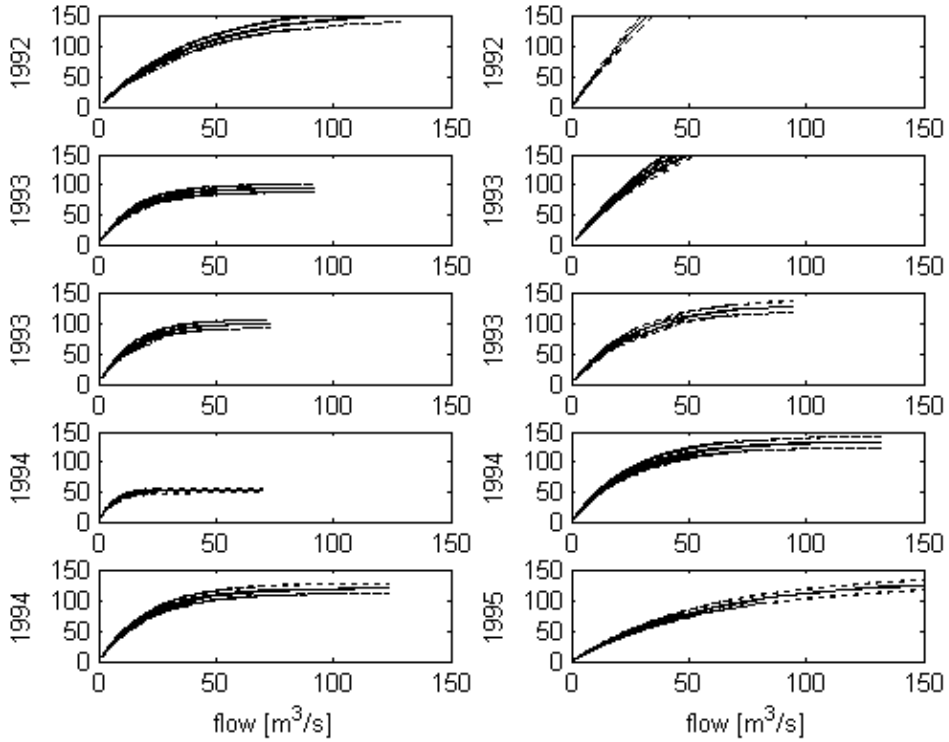

Figure A4.24a Nonlinear gains for the years 1992-1995 with 0.95 confidence bounds

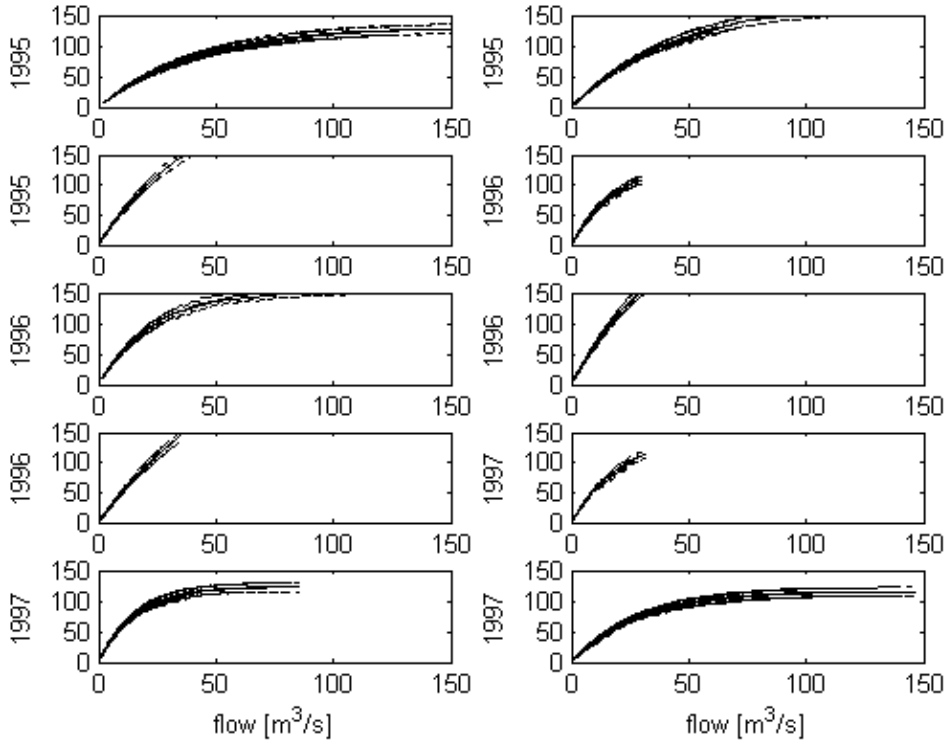

Figure A4.4b Nonlinear gains for the years 1984-2003 with 0.95 confidence bounds

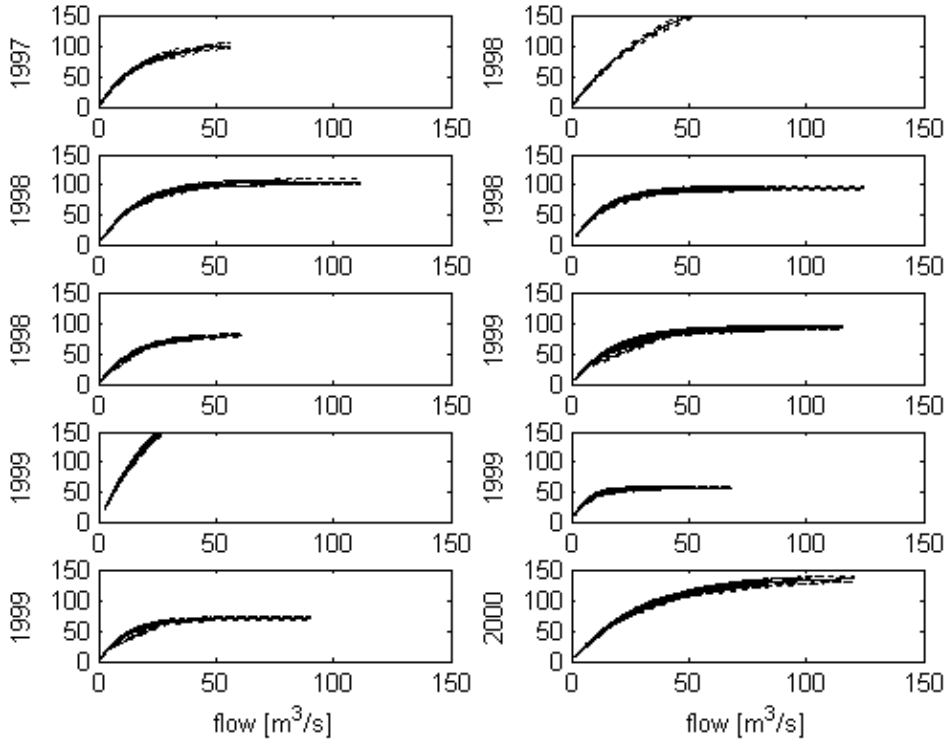

Figure A4.24c Nonlinear gains for the years 1997-2000 with 0.95 confidence bounds

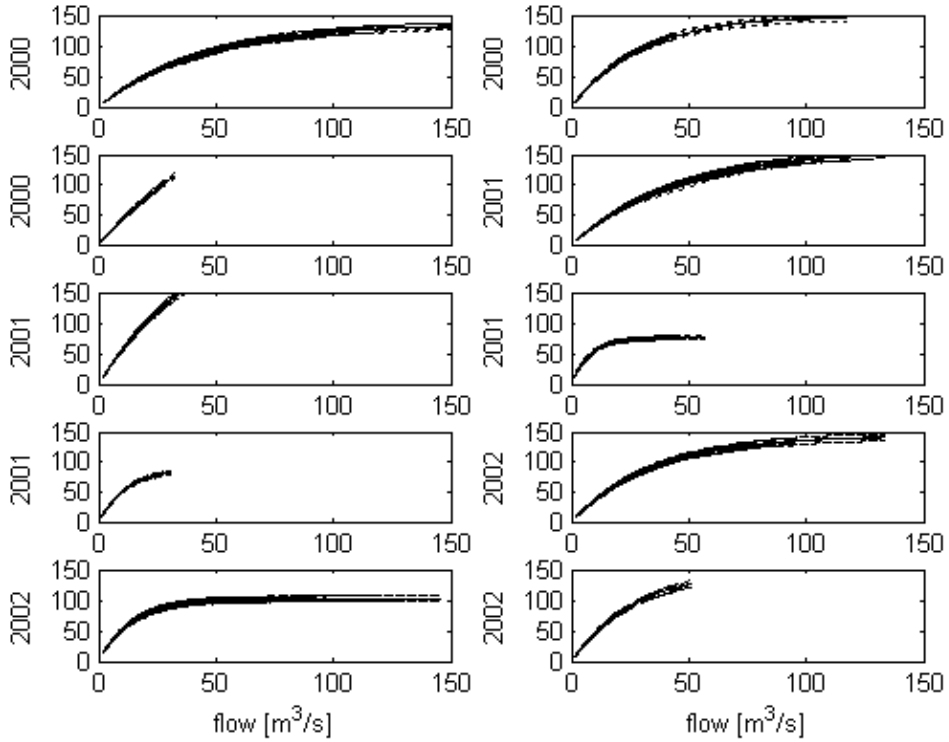

Figure A4.24d Nonlinear gains for the years 2000-2002 with 0.95 confidence bounds

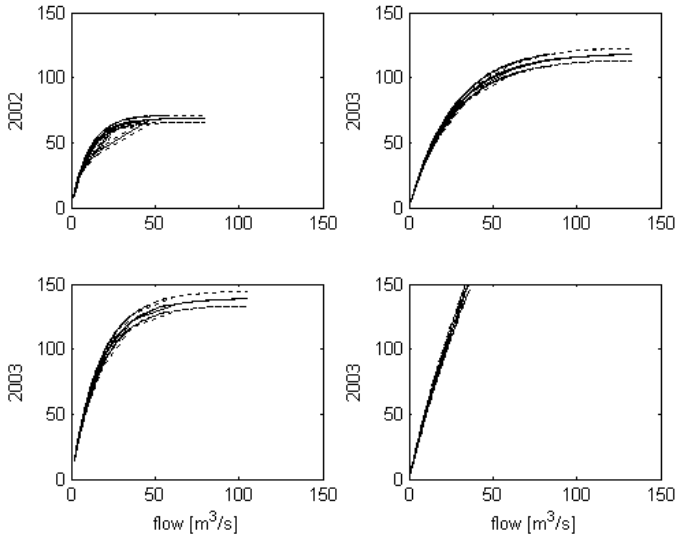

Figure A4.24e Nonlinear gains for the years 2002-2003 with 0.95 confidence bounds

A4.3.4 Analysis of DBM results for Irthing

The parameters of the models were found to vary significantly from year to year relative to the uncertainty in the values identified for each year. Results are shown for proportions between fast and slow flow components (Figure A4.25), residence times (Figure A4.27) and gains (Figure A4.28). Figure A4.26 shows the proportions between fast and slow components as a function of maximum flow. The goodness of fit values (R_T^2) of each DBM model also varied from year to year and are shown in Figure A4.30.

There is some slight tendency for a decrease of slow component proportion and an increase in fast flow proportion with time (Figure A4.25). There is no clear trend in flow proportions with maximum flow, but fast residence time decreases significantly with maximum flow in each period (Figure A4.27).

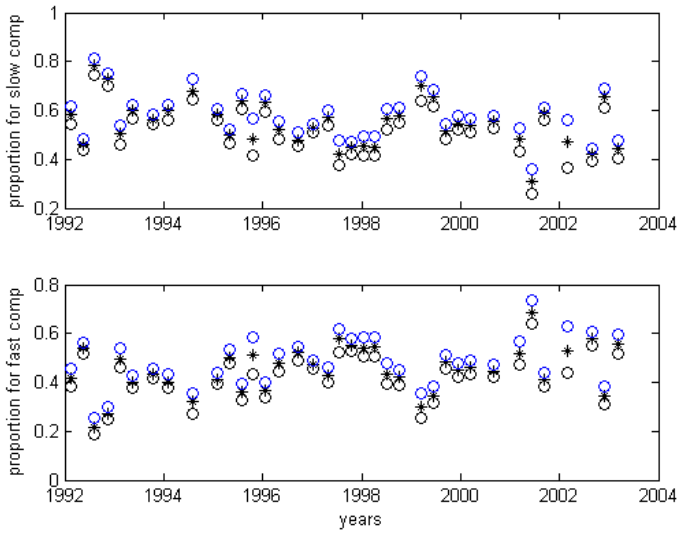

Figure A4.25 Proportions of total discharge with 0.95 confidence bounds identified for slow component (upper panel) and fast flow component (lower panel).

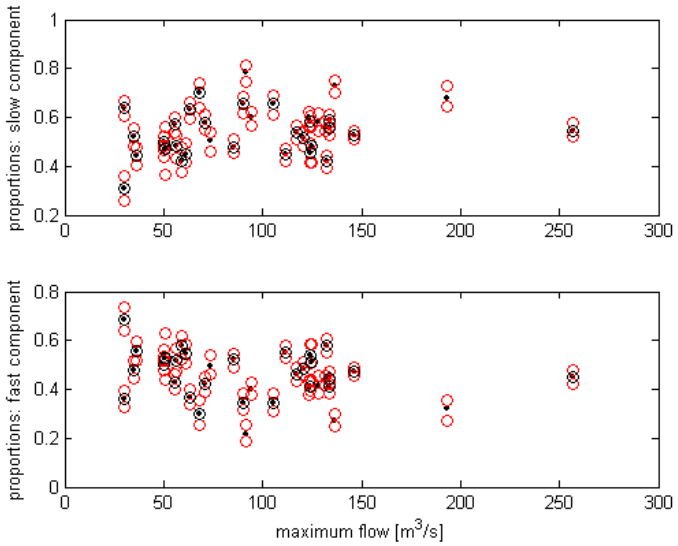

Figure A4.26 Proportions as a function of maximum flow (black dots) with 0.95 confidence bounds (red circles) against maximum flow. Black circles denote events from the years 1995-2003

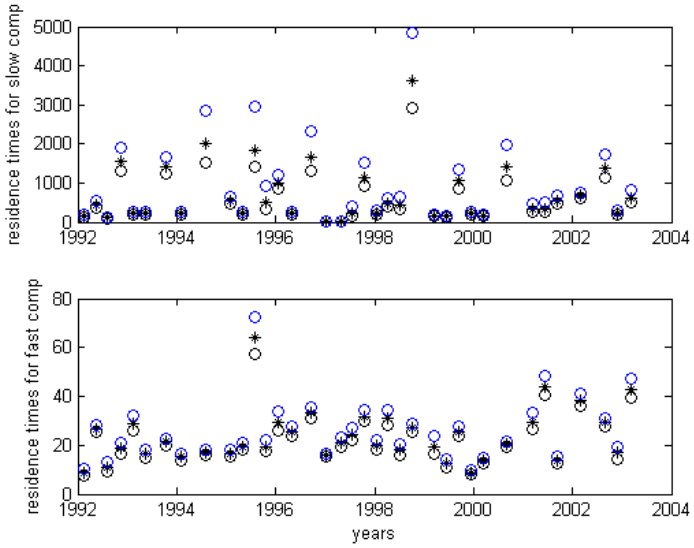

Figure A4.27 Identified residence times (hours) (as number of 15 minute time steps) with 0.95 confidence bounds for slow component (upper panel) and fast flow component (lower panel).

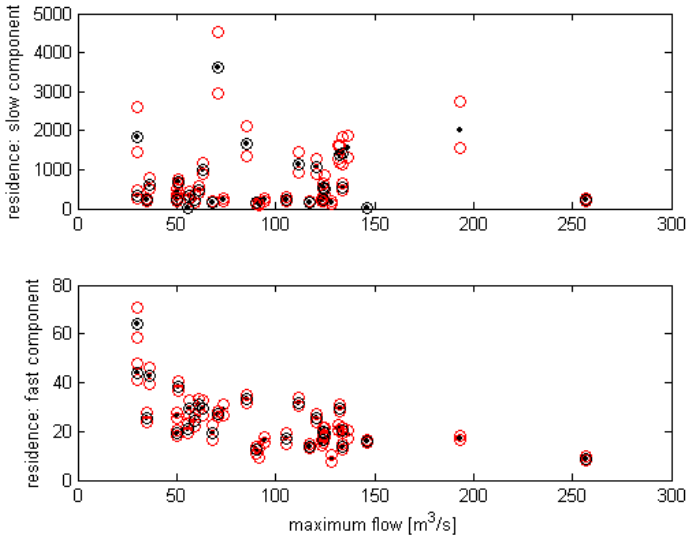

Figure A4.28 residence times (hours) as a function of maximum flow (black dots) with 0.95 confidence bounds (red circles) against maximum flow. Black circles denote events from the years 1995-2003

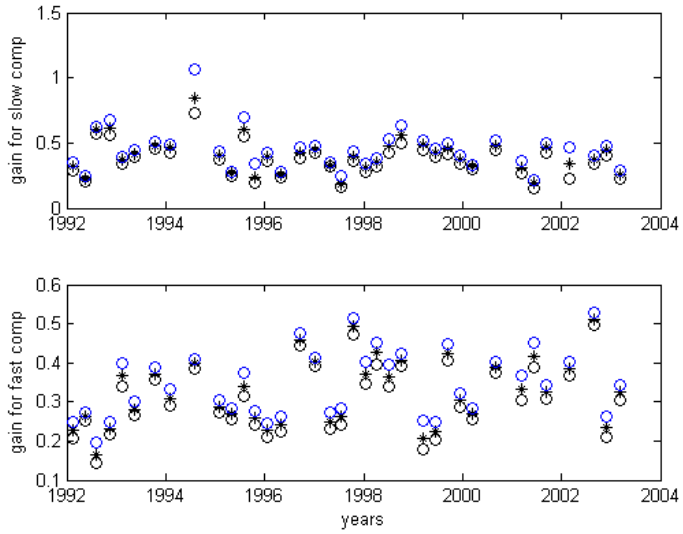

Figure A4.29 Identified gains with 0.95 confidence bounds for slow component (upper panel) and fast flow component (lower panel).

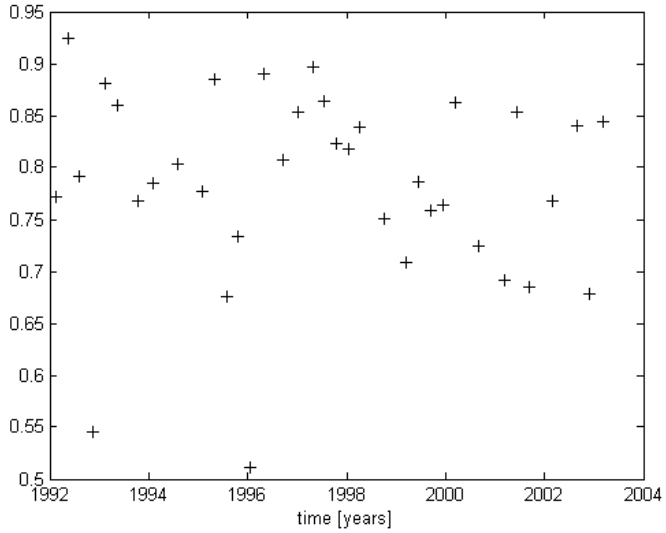

Figure A4.30 Goodness of fit R_T^2 values for DBM model for each year.

A4.4 Isle Catchment

A4.4.1 Catchment data

The flow data for the Isle Catchment (90 km^2) begin on the 01/01/1974, and end on the 02/03/2004. There are some short periods of missing values which can be easily interpolated using Captain toolbox.

There are rainfall quarterly datasets starting on the 01/01/1974 and ending at the end of 1980, one year period in 1984 and the last starting on 31/01/1995 and ending on 12/02/2003. The hourly flow and rainfall data for the 1974-1986 are shown in Figure A4.31.

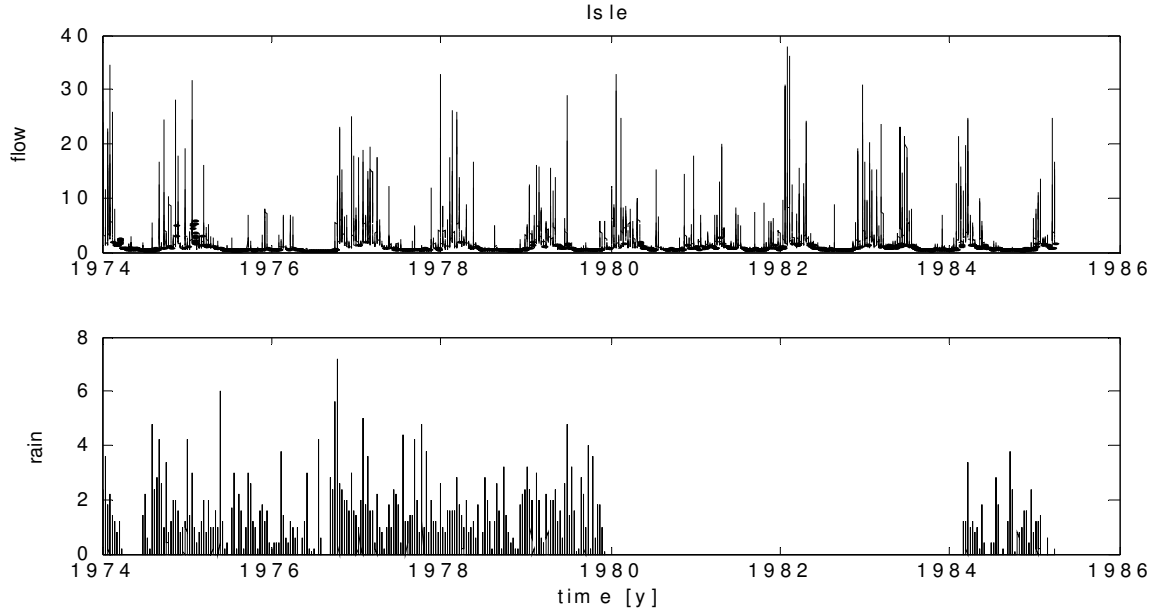

Figure A4.31 Flow (upper panel) and rainfall (lower panel) data for Isle (1974-1986)

A4.4.2 DHR Analysis

Figures A4.32 illustrates the application of the DHR method to logarithms of monthly flow and sums of monthly rainfall for the Isle. Monthly records are used in this stage of the analysis to filter out the high variability of the daily records, particularly in the rainfalls. Using the DHR methods we are looking for long term trends in the data and modelled frequency components of the data, not changes in the short term catchment dynamics. Figure A4.32 shows the identified trend in the log discharges together with 0.95 confidence bounds shown in red (upper panel) and rainfall trend with 0.95 confidence bounds (lower panel). Figure A4.33 shows the normalised trends after normalising the discharge trends as before. Based on a normal significance test, the trend in flow is significant, whereas the monthly rainfalls show no significant trend.

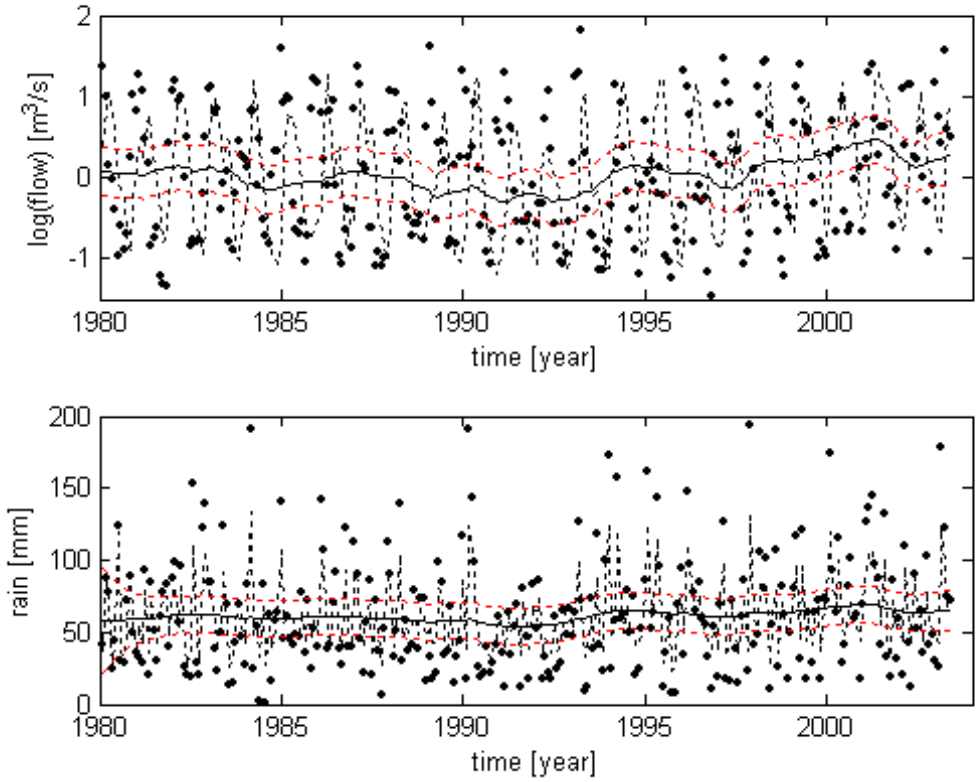

Figure A4.32 Comparison of trends for logarithm of monthly flow (upper panel) and monthly sums of rainfall (lower panel).

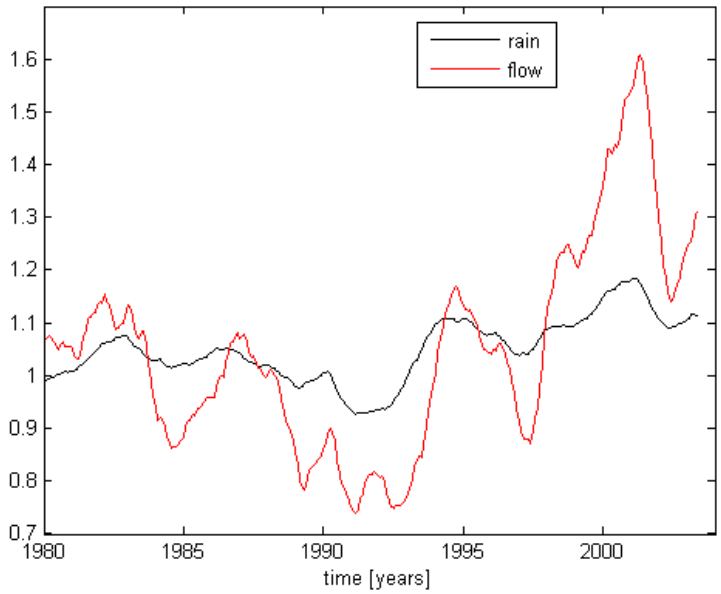

Figure A4.33 Nonstationary trends in monthly rainfall and flows in the Isle catchment scaled to equal total volumes

A4.4.3 DBM Analysis

Table A4.4 present the results of the DBM modelling of rainfall-runoff dynamics applied to the Isle catchment for higher flow Autumn-Winter periods of about 6 months long in each year. The identified transfer function model for this catchment was second order with zero delay. The estimated effective rainfall nonlinearity has an exponential shape, similar to the Axe catchment (eq. 2). The parameters of second order models, a_1, a_2, b_0, b_1 were estimated together with the effective rainfall parameter γ. The first column of the table (period) refers to the middle point of the time horizon of each event. The goodness of fit criterion R_T^2 is given in the last column and show that with the exception of 2 years, the model reproduces the rainfall-runoff dynamics well (see also Figure A4.41).

Table A4.4 Parameters of the DBM model for Isle

period	a_1	a_2	b_0	b_1	γ	R_T^2
1974.91	-1.87	0.87	0.05	-0.05	0.20	0.95
1976.11	-1.91	0.91	0.02	-0.02	0.21	0.91
1977.11	-1.88	0.88	0.04	-0.04	0.11	0.89
1978.11	-1.90	0.90	0.03	-0.03	0.16	0.65
1979.11	-1.92	0.92	0.02	-0.02	0.22	0.67
1995.38	-1.89	0.89	0.03	-0.03	0.20	0.92
1996.12	-1.90	0.90	0.04	-0.04	0.11	0.89
1997.12	-1.90	0.90	0.03	-0.03	0.22	0.92
1998.12	-1.87	0.87	0.05	-0.05	0.18	0.94
1999.12	-1.86	0.86	0.03	-0.03	0.16	0.50
2000.20	-1.83	0.83	0.06	-0.06	0.15	0.96
2001.12	-1.81	0.81	0.06	-0.06	0.15	0.92
2002.12	-1.84	0.84	0.04	-0.04	0.11	0.82
2002.99	-1.83	0.83	0.05	-0.05	0.24	0.83

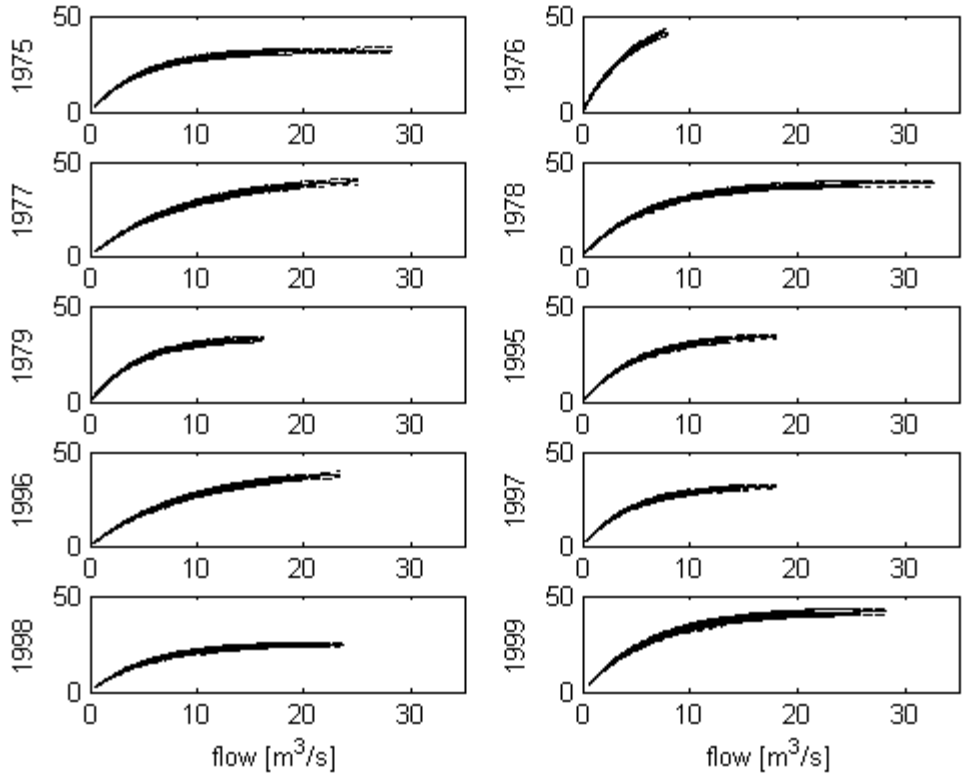

Figure A4.34a. Nonlinear gains for the years 1974-1999 with 0.95 confidence bounds

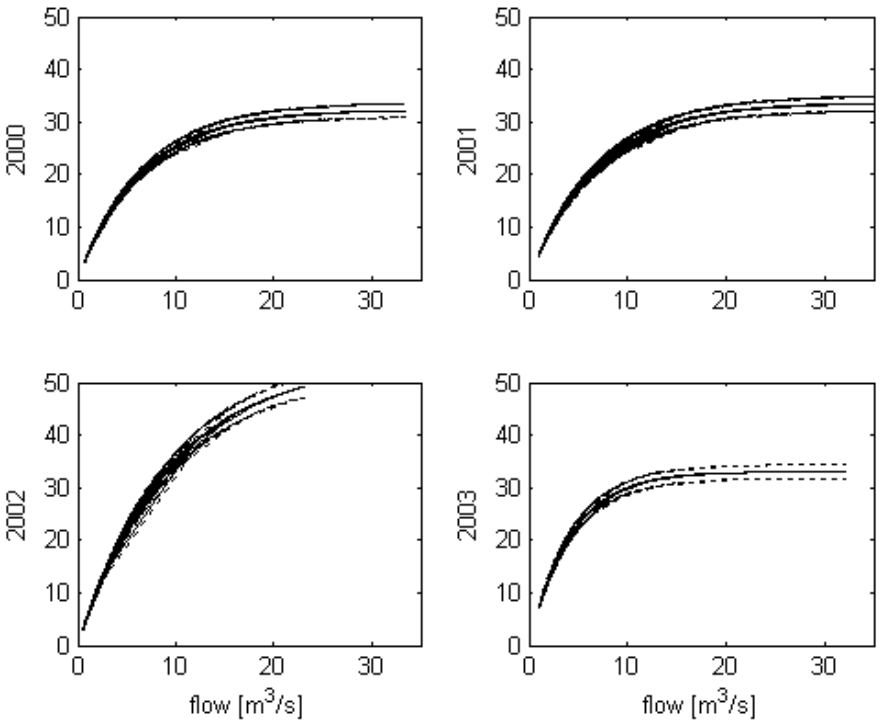

Figure A4.34b. Nonlinear gains for the years 2000-2003 with 0.95 confidence bounds

A4.4.4 Analysis of DBM Results for Isle

The parameters of the models were found to vary significantly from year to year relative to the uncertainty in the values identified for each year. Results are shown for proportions between fast and slow flow components (Figure A4.35), residence times (Figure A4.37) and gains (Figure A4.38). Figure A4.36 shows the proportions between fast and slow components as a function of maximum flow. Figure A4.38 shows the residence times for fast and slow catchment response components as a function of maximum flow and Figure A4.40 presents gains versus maximum flows. The goodness of fit values (R_T^2) of each DBM model also varied from year to year and are shown in Figure A4.41.

These analyses show little evidence of changes in the derived variables of the DBM models with time except, perhaps, in the fast and slow residence times (Figures A4.37). Fast and slow flow proportions (Figure A4.36), fast component residence times (Figure A4.38) and (less clearly) fast and slow gains (Figure A4.39) show changes with maximum flow.

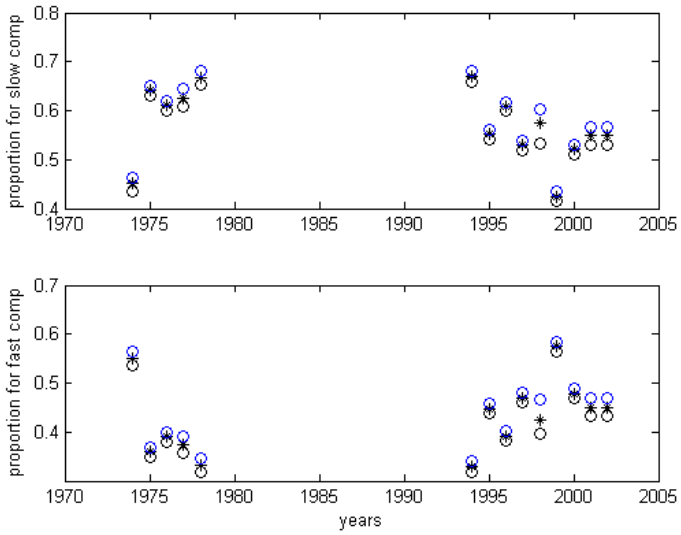

Figure A4.35. Proportions of total discharge with 0.95 confidence bounds identified for slow component (upper panel) and fast flow component (lower panel).

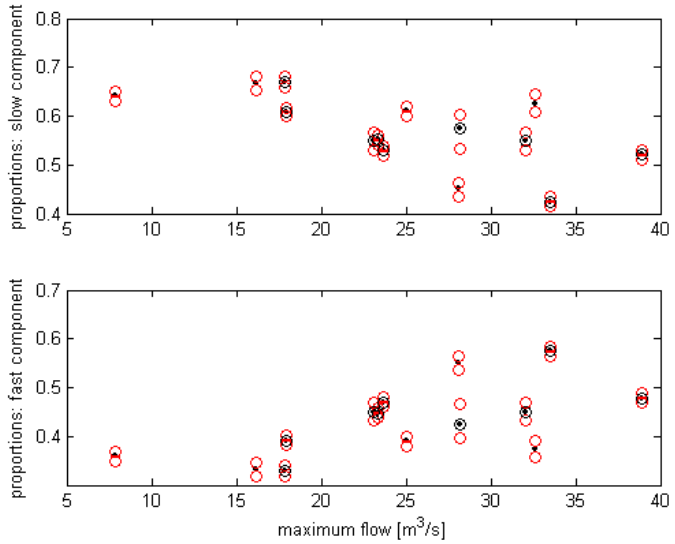

Figure A4.36. Proportions as a function of maximum flow (black dots) with 0.95 confidence bounds (red circles). Black circles denote events from the years 1995-2003

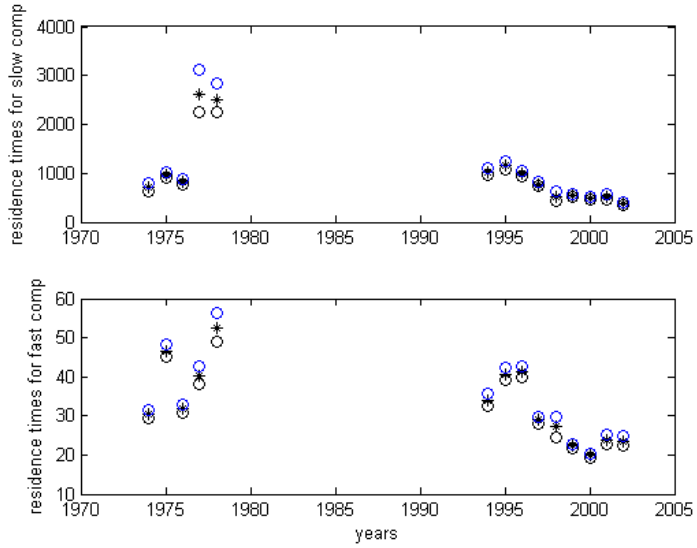

Figure A4.37. Identified residence times (as number of 15 minute time steps) with 0.95 confidence bounds for slow component (upper panel) and fast flow component (lower panel).

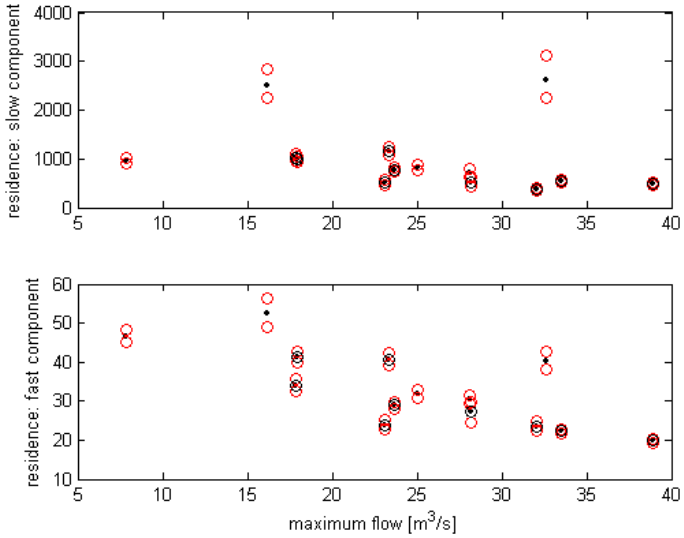

Figure A4.38 Residence times (15min intervals) as a function of maximum flow (black dots) with 0.95 confidence bounds (red circles). Black circles denote events from the years 1995-2003

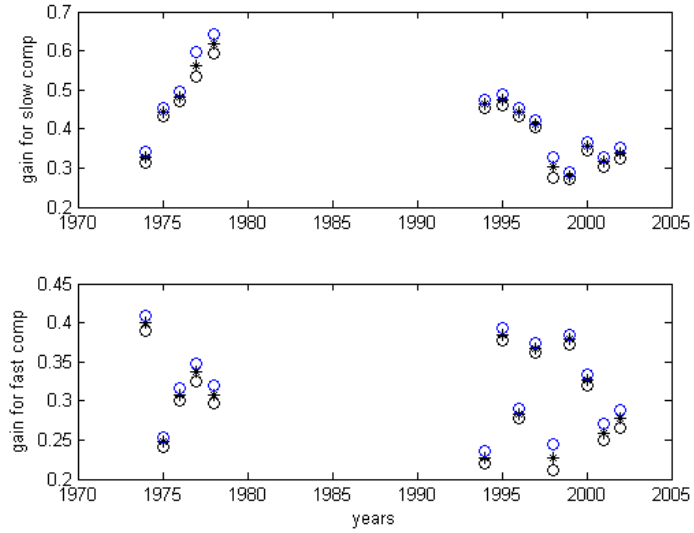

Figure A4.39 Identified gains with 0.95 confidence bounds for slow component (upper panel) and fast flow component (lower panel).

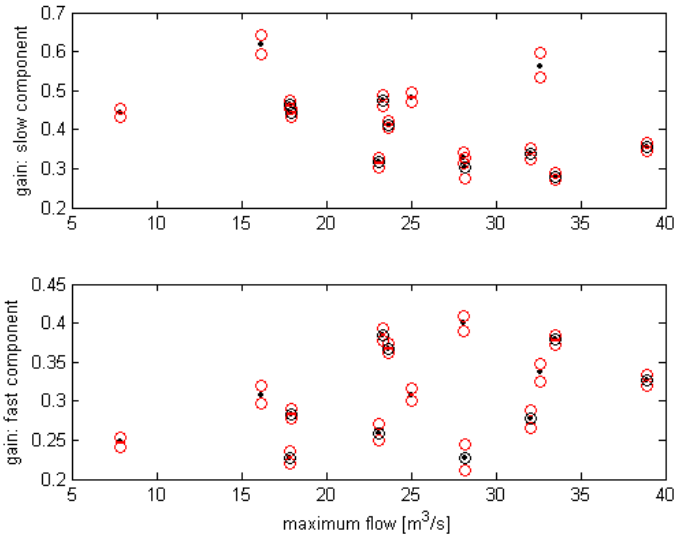

Figure A4.40 Gains as a function of maximum flow (black dots) with 0.95 confidence bounds (red circles). Black circles denote events from the years 1995-2003

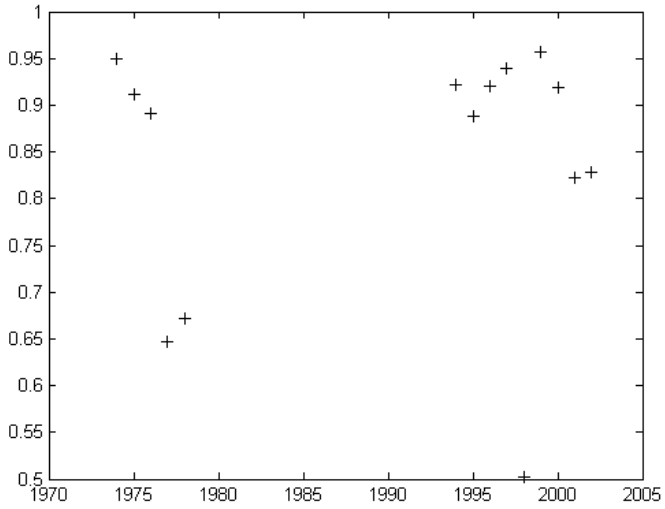

Figure A4.41. Goodness of fit for the models

A4.5 Lugg Catchment

A4.5.1 Catchment data

The flow data for the Lugg catchment (203 km^2) begin on the 01/04/1981 00:00, and end on the 22/02/2004 08:30. There are some longer periods of missing values at the beginning of 1983- 1984. Shorter than a day missing periods can be easily interpolated using the CAPTAIN toolbox.

There are three rainfall datasets starting on the 07/10/1988 00:00, 25/03/1991 00:00 and 01/01/1993 00:00 and ending on the 10/08/2003 13:00.

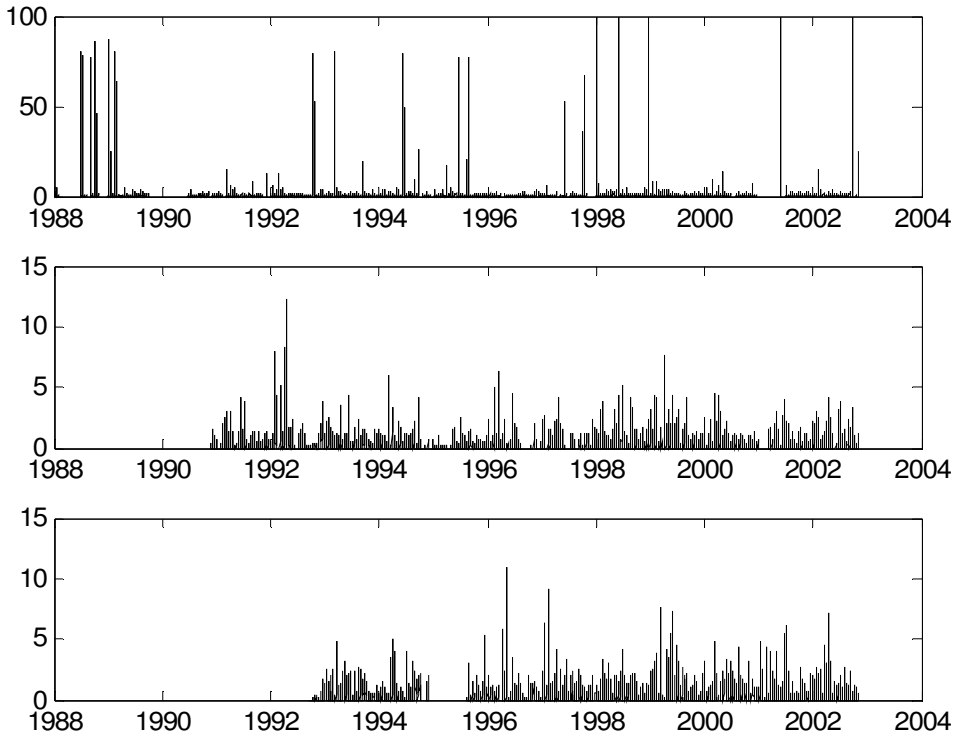

Figure A4.42. Hourly rainfall data, Lugg, three rain gauge stations.

The hourly rainfall measurements for Lugg for three rain gauge stations are shown in Figure A4.42. The first data set (upper panel from Figure A4.42) is not compatible with the datasets shown in the two lower panels, nor with the flow values shown in Figure A4.43 Therefore it was decided to use the dataset from the middle panel, which was the

longest and gave the best modelling results, better than attempts to combine the different rainfall series.

Hourly flow data are presented in Figure A4.43.

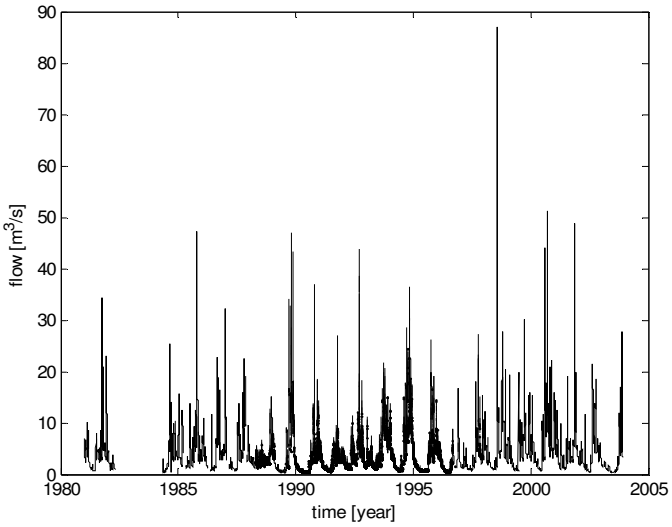

Figure A4.43. Hourly flow data, Lugg.

A4.5.2 DHR Analysis for Lugg.

Figures A4.44 illustrates the application of the DHR method to logarithms of monthly flow and sums of monthly rainfall for the Lugg. The daily records for the rainfall are converted into monthly data. Figure A4.44 shows the identified trend in the log discharges together with 0.95 confidence bounds shown in red (upper panel) and rainfall trend with 0.95 confidence bounds (lower panel). Figure A4.45 shows monthly rainfall and flow data scaled to equal total volumes.

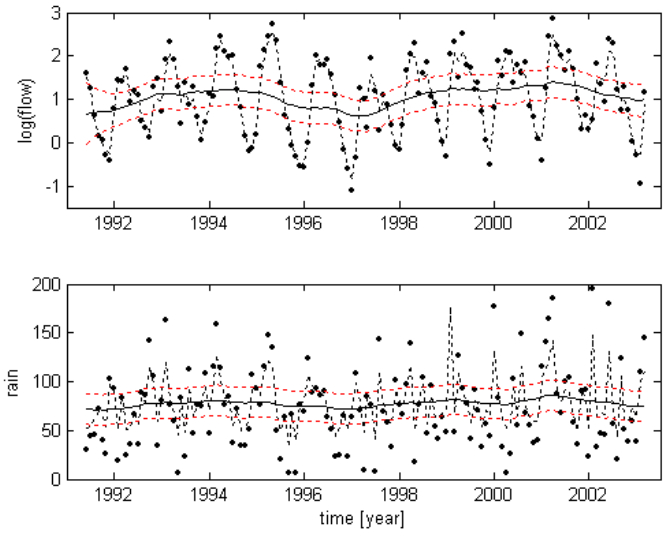

Figure A4.44 Comparison of trends for logarithm of monthly flow (upper panel) and monthly sums of rainfall (lower panel).

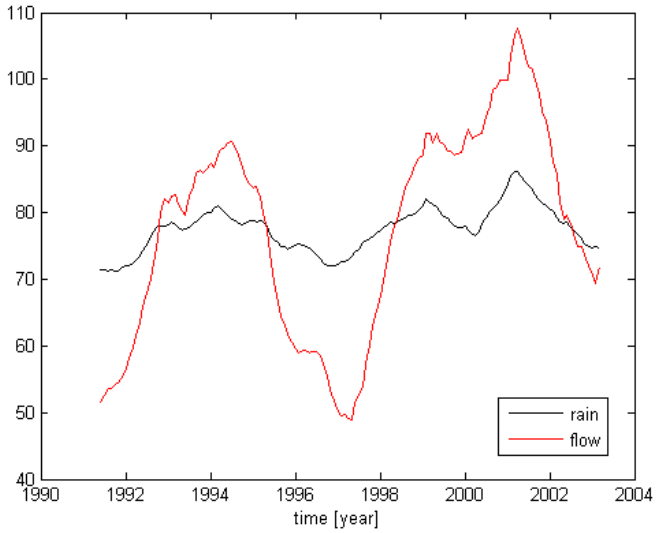

Figure A4.45 Nonstationary trends in monthly rainfall and flows in the Lugg catchment scaled to equal total volumes

The DHR trends for both rainfall and flow for the Lugg are not significant using the normal test.

A4.5.3 DBM Analysis

The results of the DBM modelling are summarised in Table A4.5. For some periods acceptable models could not be found, indicating that rainfall and flow data did not match. The estimated effective rainfall nonlinearity has an exponential shape, similar to

the Axe catchment. The parameters of second order model a_1, a_2, b_0, b_1 were estimated together with the effective rainfall parameter γ. The first column of the table (period) refers to the middle point of the time horizon of each event. The goodness of fit criterion R_T^2 is given in the last column (see also Figure A4.53).

Table A4.5. Parameters of the DBM model for Lugg

period	a_1	a_2	b_0	b_1	γ	R_T^2
1991.60	-1.98	0.98	0.00	0.00	0.00	0.90
1991.97	-1.64	0.64	0.01	-0.01	0.06	0.56
1992.80	-1.97	0.97	0.01	-0.01	0.05	0.79
1993.23	-1.97	0.97	0.01	-0.01	0.06	0.85
1993.93	-1.99	0.99	0.00	0.00	0.00	0.89
1994.89	-1.96	0.96	0.01	-0.01	0.03	0.88
1995.80	-1.97	0.97	0.01	-0.01	0.03	0.82
1996.64	-1.99	0.99	0.00	0.00	0.02	0.82
1998.54	-1.96	0.96	0.01	-0.01	0.00	0.69
1999.35	-1.99	0.99	0.00	0.00	0.02	0.76
1999.91	-1.95	0.95	0.01	-0.01	0.02	0.77
2000.56	-1.98	0.98	0.01	-0.01	0.00	0.77
2001.97	-1.94	0.94	0.02	-0.02	0.04	0.88
2002.56	-1.98	0.98	0.01	-0.01	0.04	0.86

Figure A4.46 shows the fitted nonlinearity for each of the periods analysed.

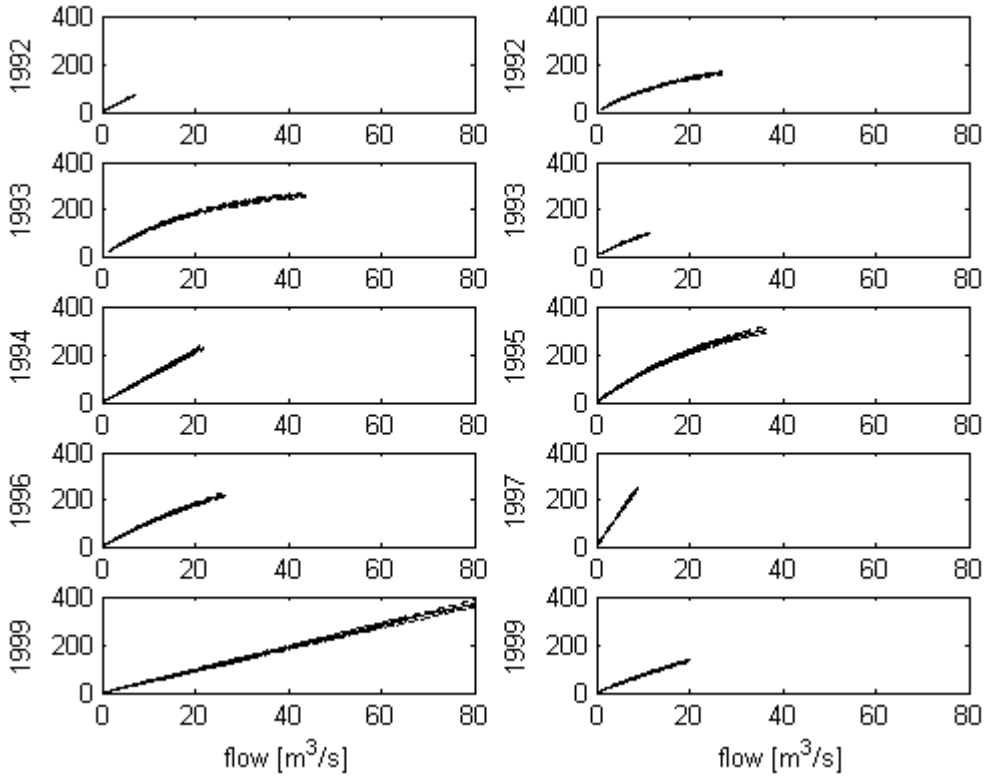

Figure A4.46a Nonlinear gains for the years 1992-1999 with 0.95 confidence bounds

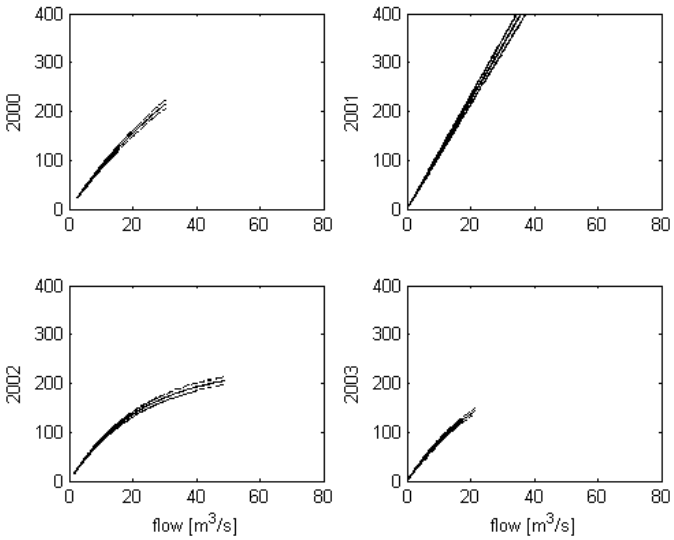

Figure A4.46b Nonlinear gains for the years 2000-2003 with 0.95 confidence bounds

A4.5.4 Analysis of DBM model results for Lugg.

There is some tendency for proportions of the fast and slow components to change with time (Figure A4.47) but no relationship with the maximum flow in each period (Figure A4.48). The residence times, presented in Figure A4.49, do show some relationship with maximum flow (Figure A4.50). Gains as a function of time are shown in Figure A4.51.

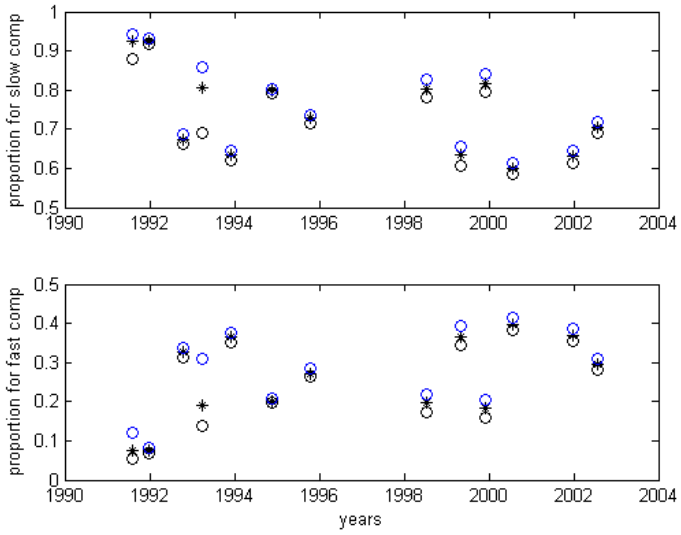

Figure A4.47 Proportions of total discharge with 0.95 confidence bounds identified for slow component (upper panel) and fast flow component (lower panel).

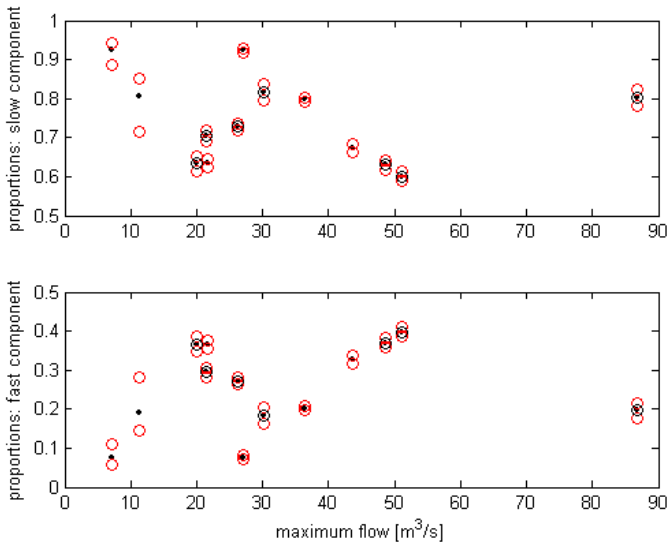

Figure A4.48 Proportions as a function of maximum flow (black dots) with 0.95 confidence bounds (red circles). Black circles denote events from the years 1995-2003

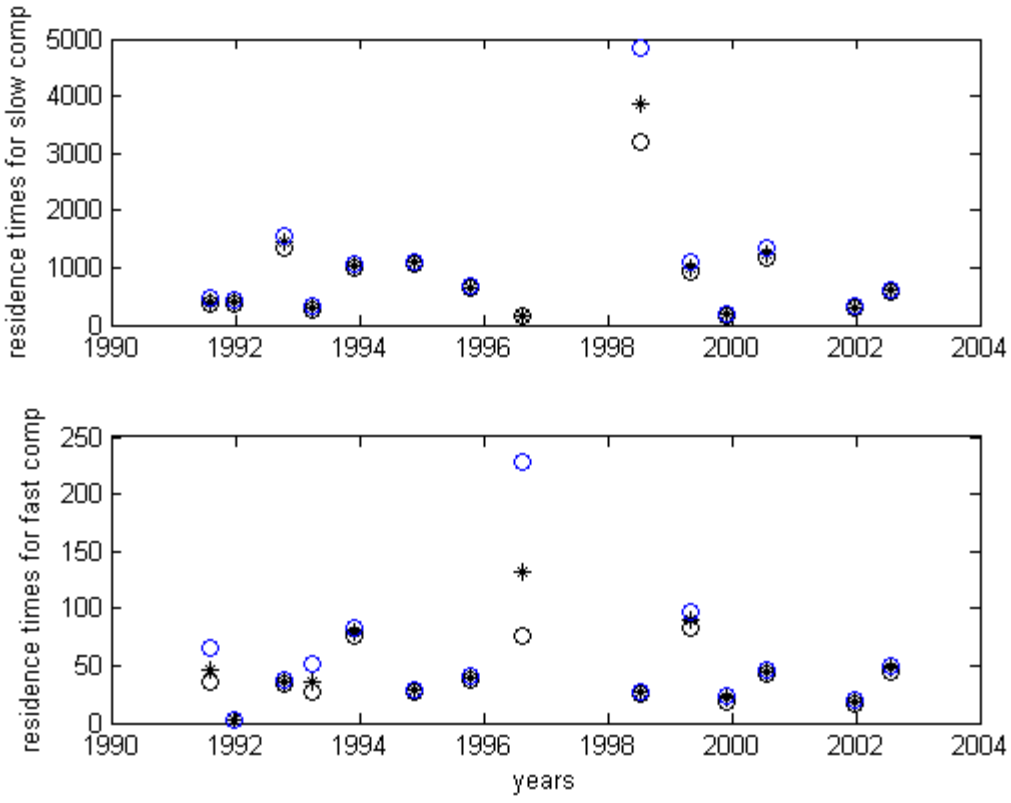

Figure A4.49 Identified residence times (hours) with 0.95 confidence bounds for slow component (upper panel) and fast flow component (lower panel).

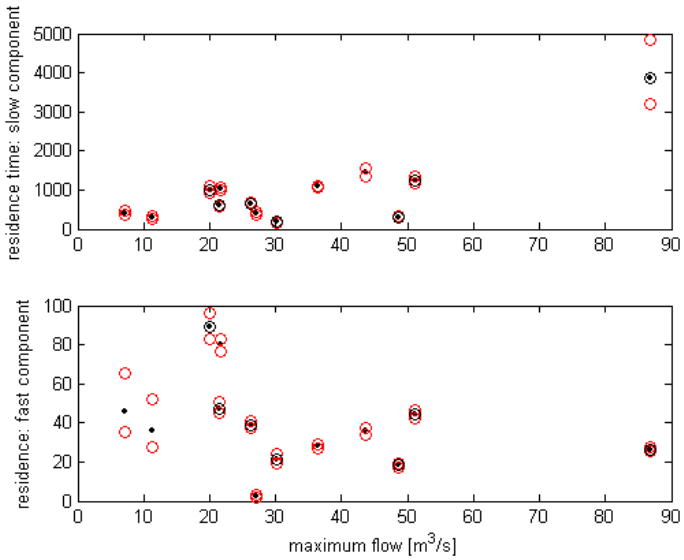

Figure A4.50 Residence times (hours) as a function of maximum flow (black dots) with 0.95 confidence bounds (red circles). Black circles denote events from the years 1995-2003

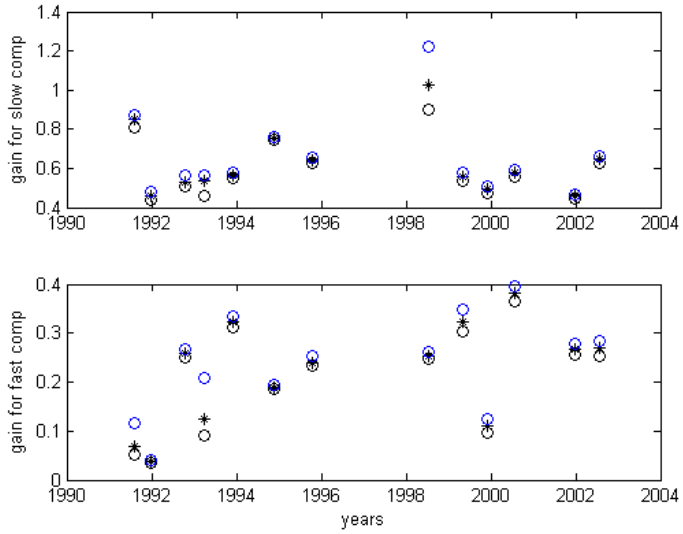

Figure A4.51 Identified gains with 0.95 confidence bounds for slow component (upper panel) and fast flow component (lower panel).

Lower panel of Figure A4.51 may indicate some tendency of the gain of the fast component to increase with time (though the 2000 period does not follow this). Figure A4.52, shows the gains as a function of maximum flow.

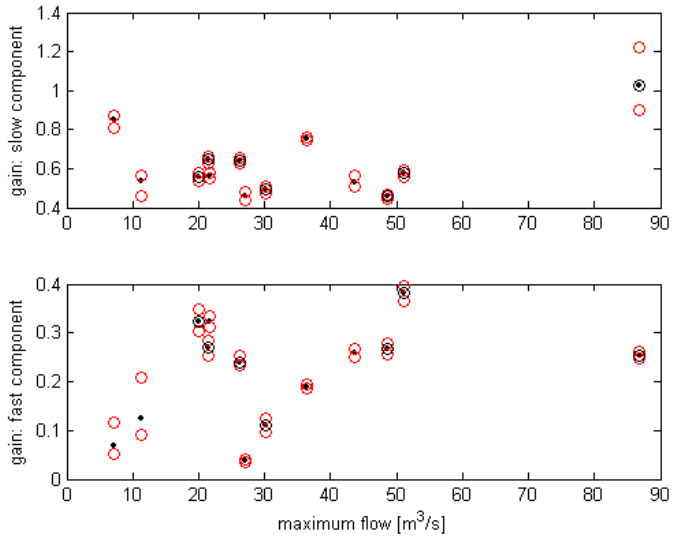

Figure A4.52 Gains as a function of maximum flow (black dots) with 0.95 confidence bounds (red circles). Black circles denote events from the years 1995-2003

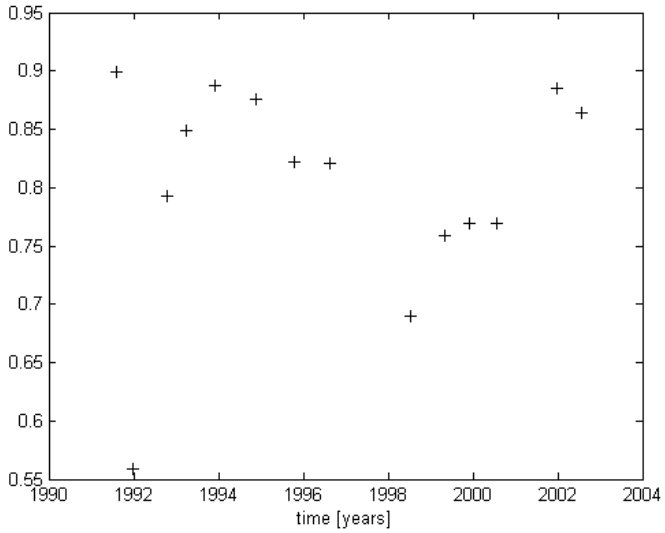

Figure A4.53. Goodness of fit for the models

A4.6 Parrett

A4.6.1 Catchment data

The Parrett catchment (75 km^2) includes the River Parrett and its main tributaries - the Tone, Isle, Cary and Yeo. The area also contains the major urban areas of Taunton, Bridgwater and Yeovil and the internationally significant Somerset Levels and Moors. It is economically, culturally, archaeologically, agriculturally, and environmentally significant, with numerous international, national and local designations of importance.

The flow data begin on the 01/04/1966 00:00, and end on the 22/02/2003 08:30. There are some longer periods of missing values at the beginning of 1983- 1984, and there is a change of raingauge site between 1986 and 1995. Figures A4.54a-b present the rainfall-flow data for Parrett catchment. Parrett flows had to be delayed by 7 hours in order to obtain good model fit.

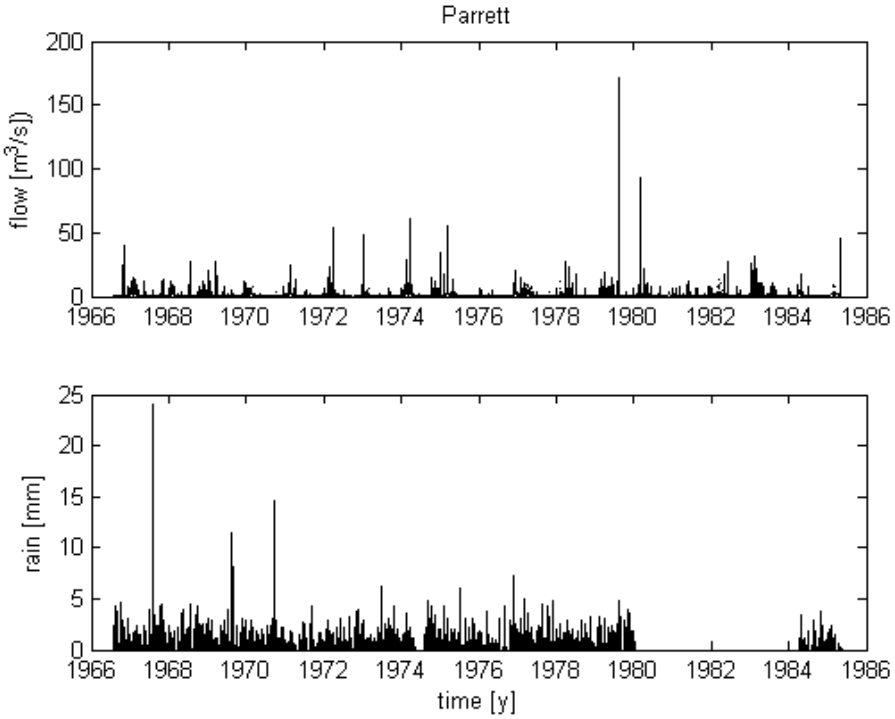

Figure A4.54a Flow (upper panel) and rainfall data for Parrett: 1966-1986.

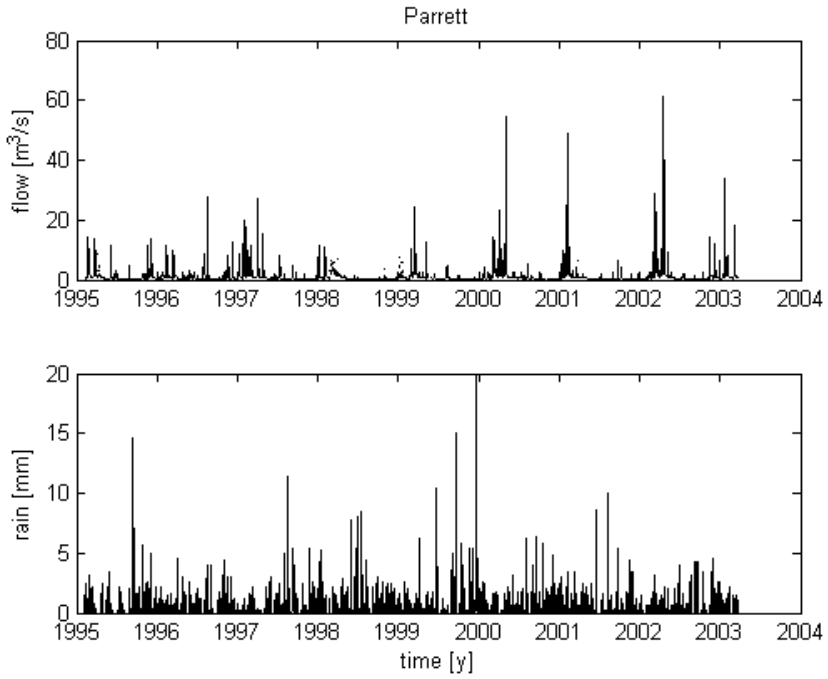

Figure A4.54b. Flow (upper panel) and rainfall data for Parrett: 1995-2003.

A4.6.2 DHR analysis

Figures A4.55 illustrates the application of the DHR method to logarithms of monthly flow and sums of monthly rainfall for the Parrett. The daily records for the rainfall are converted into monthly data. Figure A4.55 shows the identified trend in the log discharges together with 0.95 confidence bounds shown in red (upper panel) and rainfall trend with 0.95 confidence bounds (lower panel). Figure A4.56 shows the trends after scaling the discharge trend to equal total volumes as before.

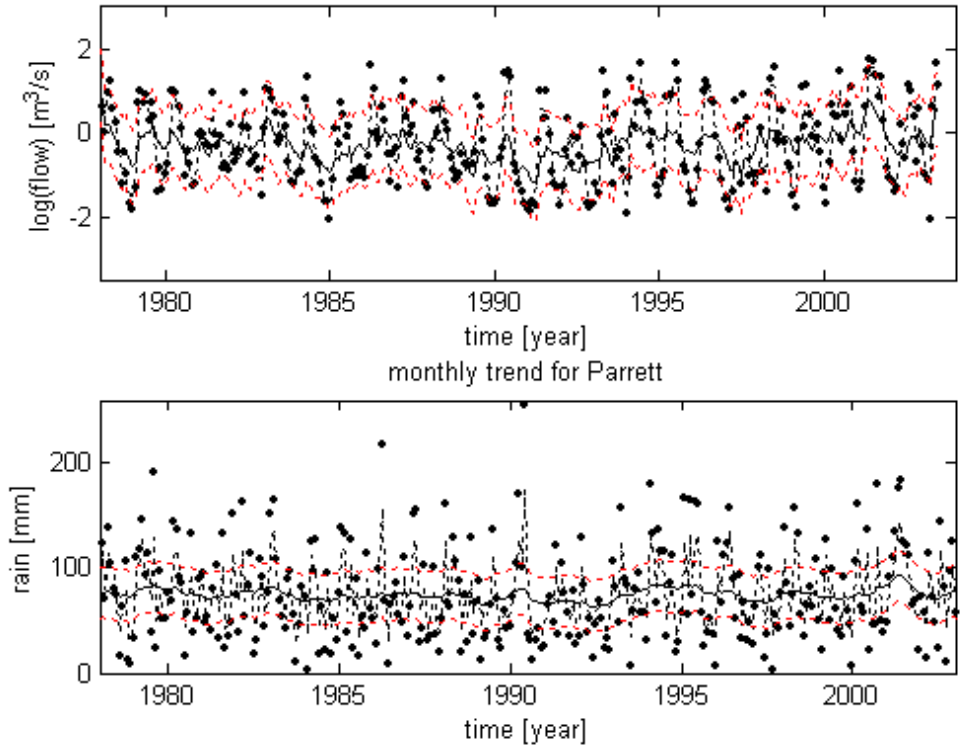

Figure A4.55. Comparison of trends for flow (upper panel) and rainfall (lower panel)

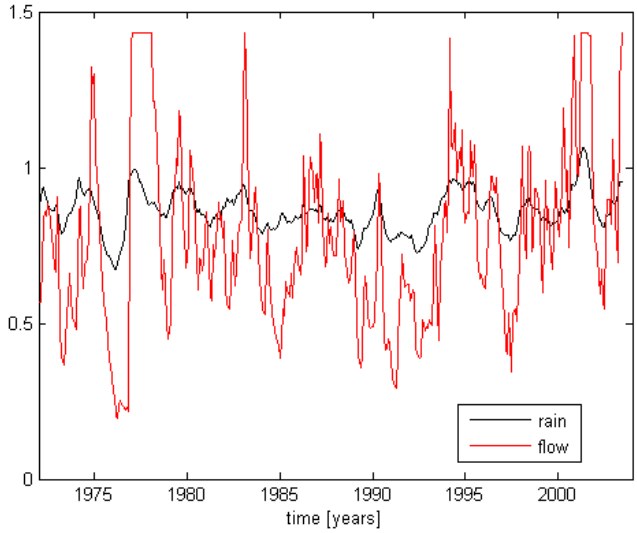

Figure A4.56. Nonstationary trends in monthly rainfall and flows in the Parrett catchment scaled to equal total volumes

The DHR trends for both rainfall and flow for the Parrett are not significant using the normal test.

A4.6.3 DBM Analysis

The time periods used for the estimation of DBM models were chosen according to the flow events during the considered time horizon of simulations. The length of time periods ranges from 500 to 3000 hours. Unfortunately, the rainfall observations for the years 1966-1988 and 1995-2003 are taken from different gauging stations and therefore the model results for these two time periods are not directly comparable.

Table A4.6 present the results of the DBM modelling of rainfall-runoff dynamics applied to the Parrett catchment for higher flow Autumn-Winter periods of about 6 months long in each year. The identified transfer function model for this catchment was second order with zero delay. The estimated effective rainfall nonlinearity has an exponential shape, similar to the Axe catchment. The parameters of second order models a_1, a_2, b_0, b_1 were estimated together with the effective rainfall parameter γ. The first column of the table (period) refers to the middle point of the time horizon of each event. The goodness of fit criterion R_T^2 is given in the last column (see also Figure A4.63). As mentioned before, the flow records had to be delayed by 7 hours in order to obtain rainfall-flow relationship. The identified nonlinearities for each simulated period are shown in Figure A4.57

Table A4.6 Parameters of the DBM second order model for Parrett.

period	a_1	a_2	b_0	b_1	γ	R_T^2
1967.07	-1.88	0.88	0.04	-0.04	0.09	0.86
1967.36	-1.89	0.89	0.03	-0.03	0.14	0.91
1967.95	-1.87	0.87	0.03	-0.03	0.01	0.86
1968.27	-1.87	0.87	0.02	-0.02	0.00	0.89
1968.62	-1.18	0.25	0.02	0.01	0.08	0.93
1968.97	-1.88	0.88	0.04	-0.04	0.12	0.82
1969.31	-1.85	0.85	0.05	-0.04	0.04	0.90
1969.94	-1.88	0.88	0.04	-0.04	0.00	0.83
1971.16	-1.86	0.87	0.04	-0.04	0.05	0.89
1972.72	-1.88	0.88	0.02	-0.02	0.00	0.85
1973.68	-1.89	0.89	0.03	-0.03	0.00	0.83
1974.02	-1.85	0.85	0.05	-0.05	0.17	0.87
1974.31	-1.60	0.61	0.11	-0.11	0.03	0.92
1974.94	-1.88	0.88	0.05	-0.05	0.03	0.83
1975.29	-1.21	0.25	0.13	-0.11	0.12	0.81
1976.33	-1.87	0.87	0.02	-0.02	0.21	0.92
1976.91	-1.87	0.87	0.05	-0.05	0.00	0.85
1978.54	-1.85	0.85	0.04	-0.04	0.20	0.94
1978.87	-1.82	0.83	0.03	-0.02	0.60	0.91
1979.43	-1.85	0.86	0.04	-0.04	0.09	0.86
1995.30	-1.91	0.91	0.06	-0.06	0.15	0.90
1995.65	-1.83	0.84	0.09	-0.09	0.00	0.91
1995.92	-1.92	0.92	0.06	-0.06	0.07	0.80
1996.30	-1.89	0.90	0.05	-0.05	0.06	0.93

1996.54	-1.79	0.80	0.03	-0.03	2.20	0.84
1996.78	-1.92	0.92	0.06	-0.05	0.20	0.92
1997.07	-1.90	0.90	0.07	-0.06	0.24	0.94
1997.32	-1.77	0.78	0.05	-0.04	0.13	0.88
1997.60	-1.91	0.91	0.06	-0.06	0.27	0.95
1997.90	-1.90	0.90	0.08	-0.08	0.25	0.89
1998.17	-1.87	0.87	0.07	-0.07	0.14	0.84
1998.41	-1.92	0.92	0.03	-0.02	0.36	0.71
1998.69	-1.88	0.89	0.09	-0.08	0.37	0.88
1999.27	-1.89	0.89	0.05	-0.04	0.00	0.87
1999.75	-1.89	0.90	0.07	-0.07	0.05	0.94
1999.93	-1.85	0.86	0.09	-0.09	0.10	0.90
2000.18	-1.89	0.89	0.07	-0.07	0.25	0.90
2000.46	-1.75	0.77	0.05	-0.05	0.00	0.81
2000.65	-1.89	0.89	0.08	-0.08	0.16	0.85
2000.90	-1.83	0.84	0.11	-0.10	0.26	0.70
2001.25	-1.88	0.89	0.08	-0.07	0.08	0.91
2001.51	-1.58	0.62	0.05	-0.04	0.60	0.91
2001.77	-1.89	0.89	0.06	-0.05	0.19	0.80
2002.11	-1.91	0.91	0.06	-0.06	0.14	0.86
2002.34	-1.90	0.90	0.07	-0.07	0.00	0.78
2002.51	-1.95	0.95	0.01	-0.01	0.00	0.66
2002.77	-1.93	0.93	0.05	-0.05	0.18	0.70

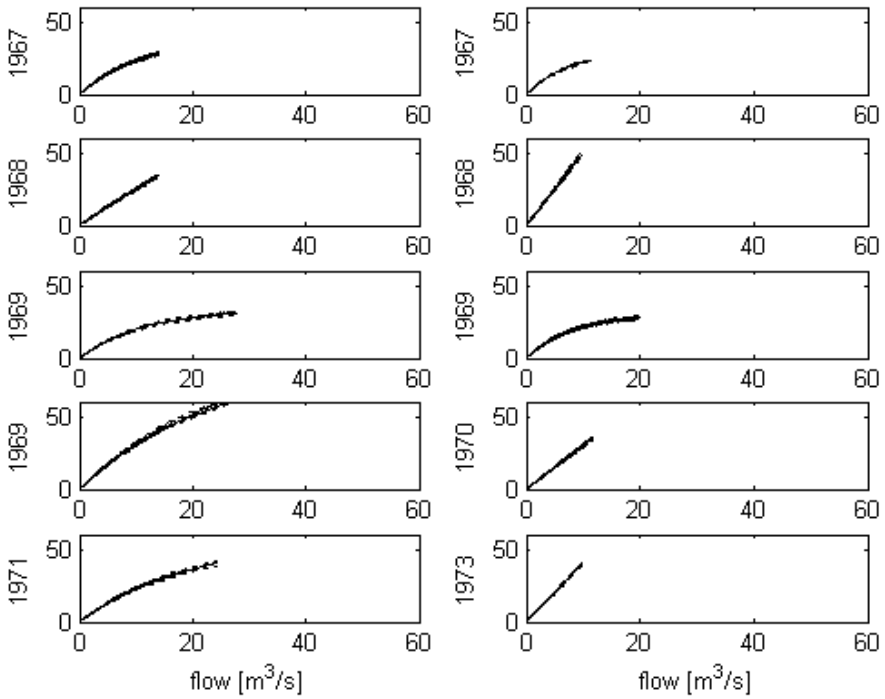

Figure A4.57a Nonlinear gains for the periods in years 1967-1973 with 0.95 confidence bounds

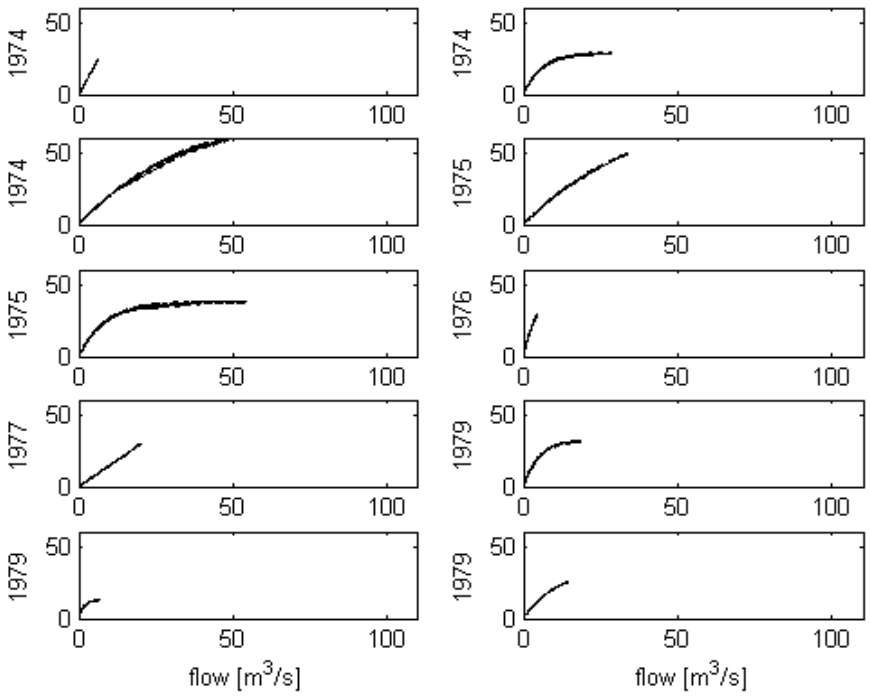

Figure A4.57b Nonlinear gains for the periods in years 1974-1979 with 0.95 confidence bounds

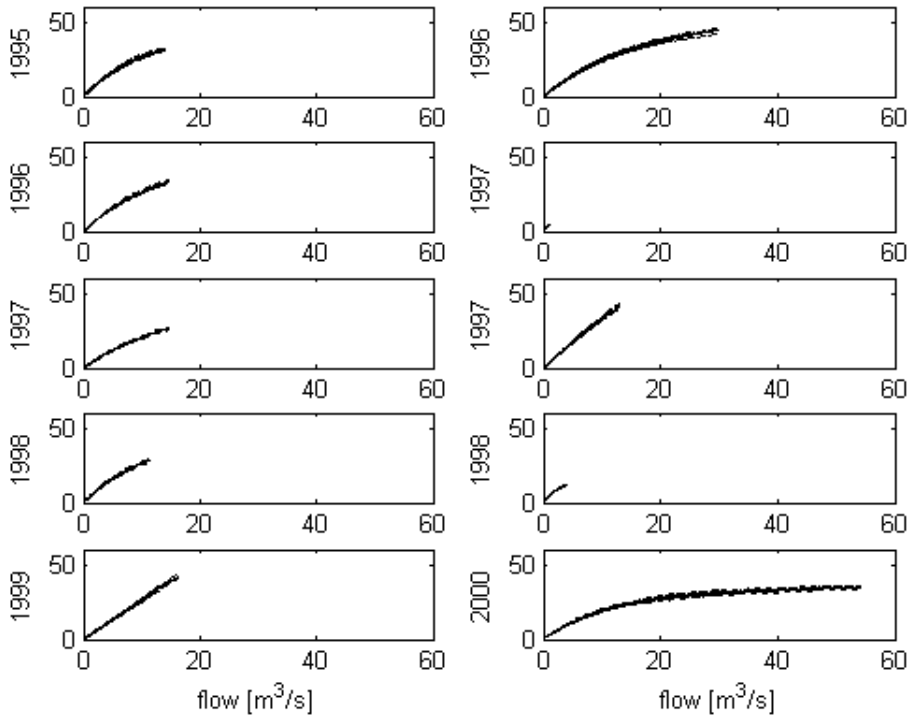

Figure A4.57c Nonlinear gains for the periods in years 1995-2000 with 0.95 confidence bounds

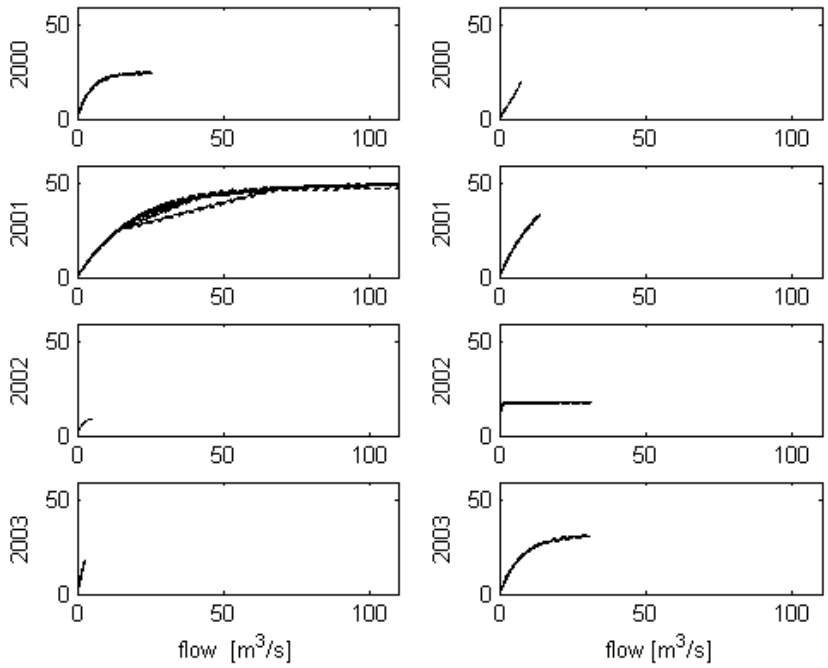

Figure A4.57d Nonlinear gains for the periods in years 2000-2003 with 0.95 confidence bounds

A4.6.4 Analysis of DBM model results for Parrett

For the River Parrett it seems as if variability between years dominates any apparent changes in the response characteristics for proportions, gains and residence time parameters. The proportions as a function of time are presented in Figure A4.58 and Figure A4.59 shows the same propotions as a function of maximum flow. Residence times are shown in Figures A4.60 and A4.61 and gains as a function of time are presented in Figure A4.62. Figure A4.63 shows the goodness of fit for the estimated models.

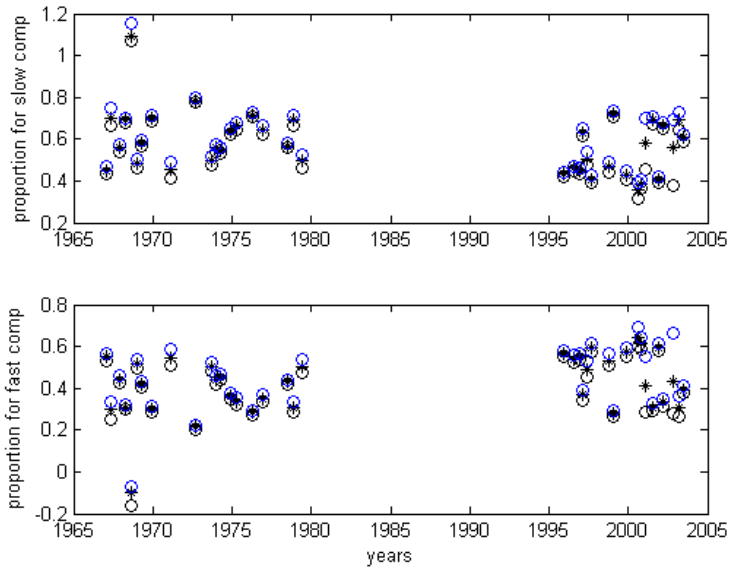

Figure A4.58 Proportions of total discharge with 0.95 confidence bounds identified for slow component (upper panel) and fast flow component (lower panel).

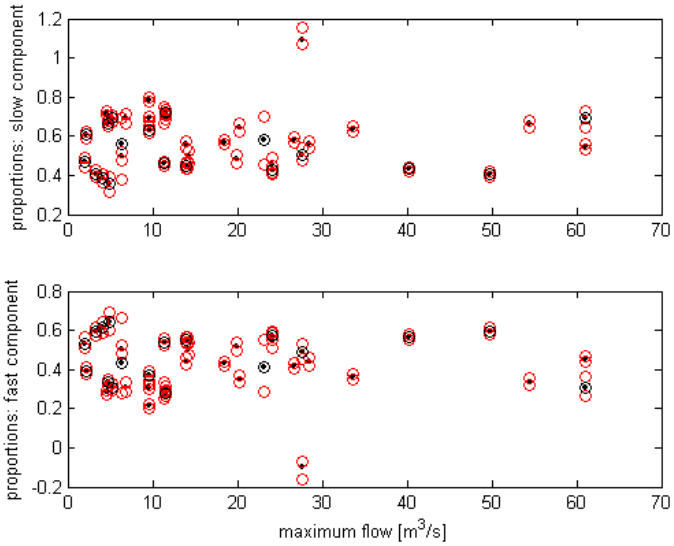

Figure A4.59 Proportions as a function of maximum flow (black dots) with 0.95 confidence bounds (red circles). Black circles denote events from the years 1997-2003

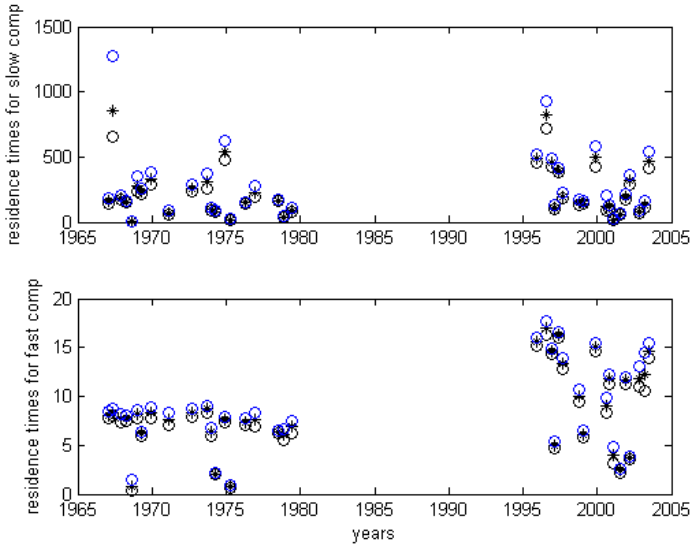

Figure A4.60 Identified residence times (hours) with 0.95 confidence bounds for slow component (upper panel) and fast flow component (lower panel).

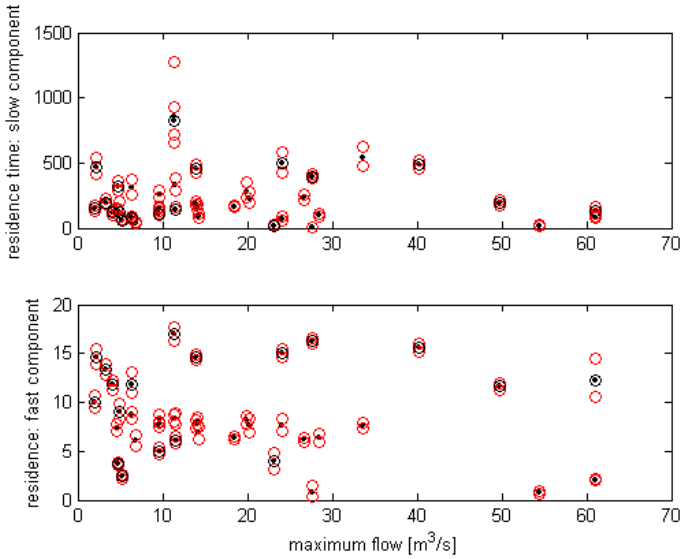

Figure A4.61 Residence times (hours) as a function of maximum flow (black dots) with 0.95 confidence bounds (red circles). Black circles denote events from the years 1997-2003

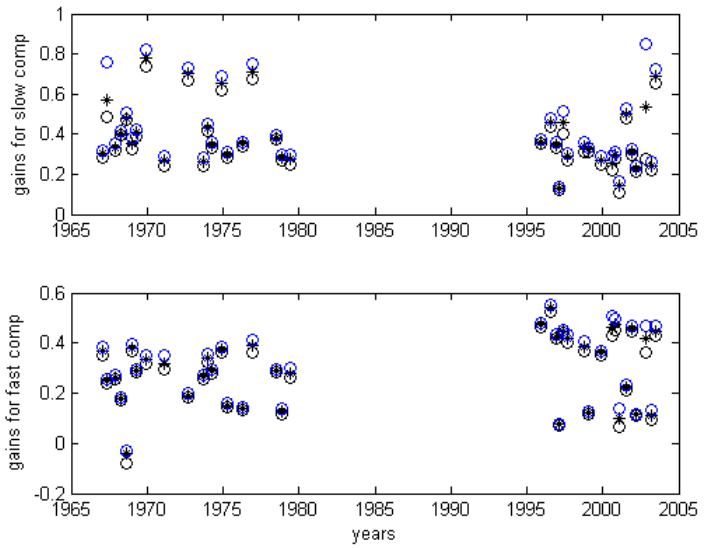

Figure A4.62 Identified gains with 0.95 confidence bounds for slow component (upper panel) and fast flow component (lower panel).

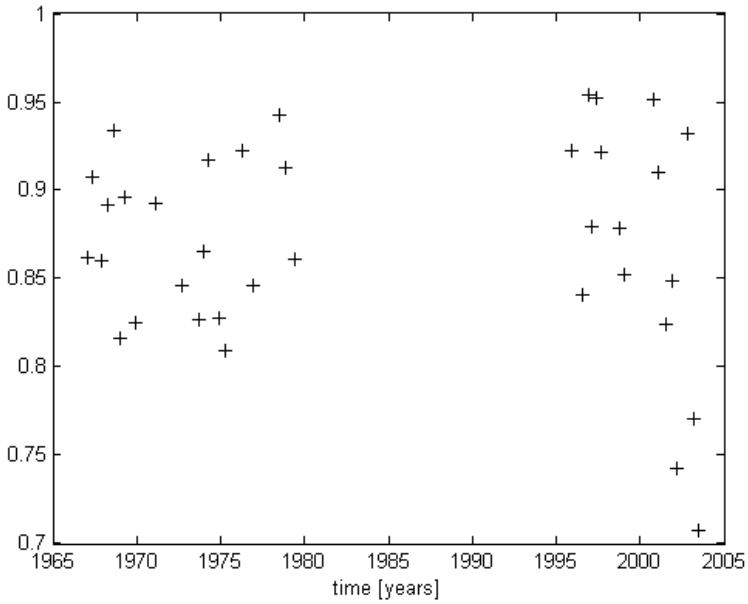

Figure A4.63. Goodness of fit for the models

A4.7 Teme

A4.7.1 Catchment data.

The Teme catchment (1135 km^2) is a sub-catchment of the River Severn. The catchment area is 1135 km^2 to the gauging station at Tenbury. The geology is mainly Palaeozoic sediments with Pre-Cambrian crystalline rocks of the Longmynd series. The catchment is relatively drift free with some valley gravels and boulder clay in the lower reaches. Forestry, grazing. Digital flow measurements start on the 30.12.1969, end on the 30.09.2003. Rainfall records start in the 1986 and end in 2006.

Flow records for Teme are shown in the upper panel of Figure A4.64, lower panel shows relevant rainfall records. Apart from the missing rainfall observations in the years 1997-2000, there are no major problems with these datasets.

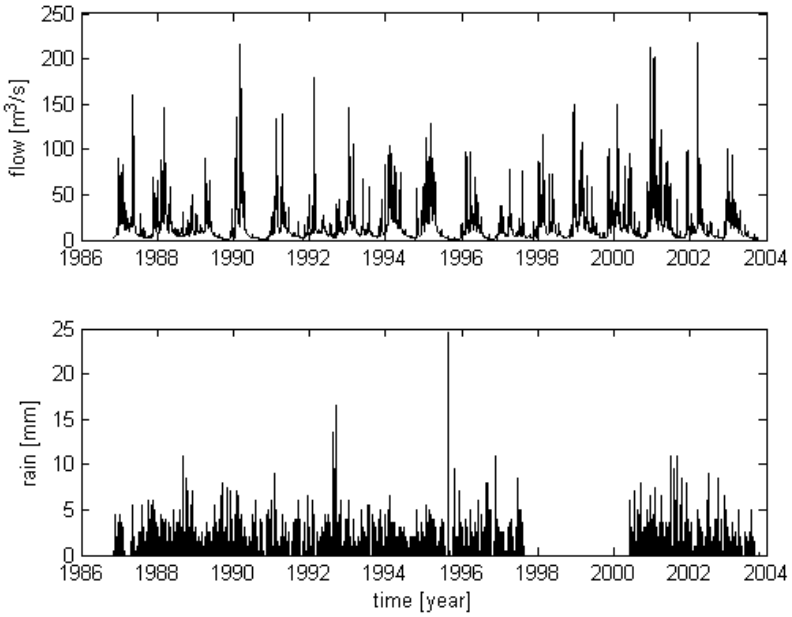

Figure A4.64 Flow (upper panel) and rainfall (lower panel) for Teme.

A4.7.2 DHR analysis

Figures A4.65 illustrates the application of the DHR method to logarithms of monthly flow and sums of monthly rainfall for the Teme. The daily records for the rainfall are converted into monthly data. Figure A4.65 shows the identified trend in the log discharges together with 0.95 confidence bounds shown in red (upper panel) and rainfall trend with 0.95 confidence bounds (lower panel). Figure A4.66 shows the trends for the rainfall and discharge scaled to equal total volumes as before.

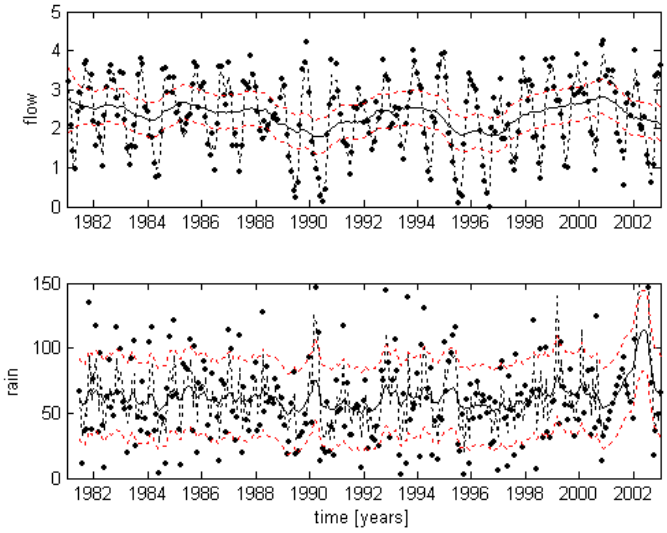

Figure A4.65 Comparison of trends for flow (upper panel) and rainfall (lower panel)

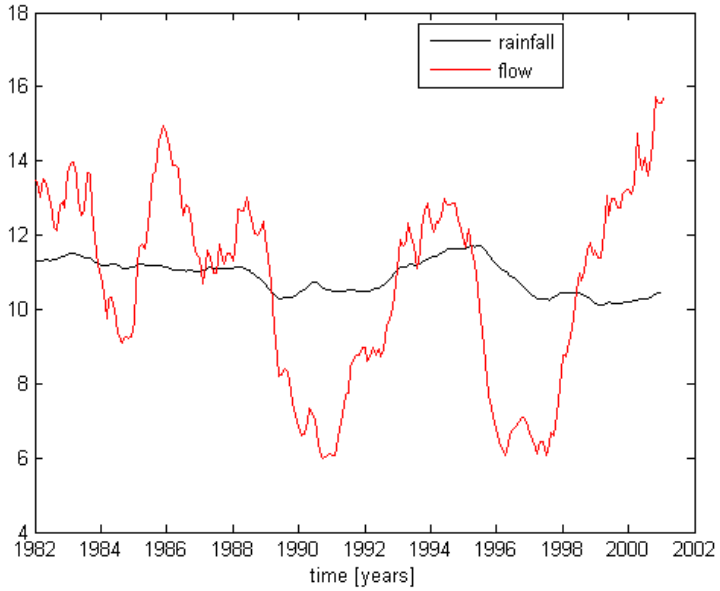

Figure A4.66 Nonstationary trends in monthly rainfall and flows in the Teme catchment scaled to equal total volumes

The DHR trends for both rainfall and flow for the Teme are not significant using the normal test.

A4.7.3 DBM Analysis

The typical best linear catchment model has second order structure [2 2 0]. Those years which are not listed in the table had very bad STF model fit (below 0.4). As a result, the number of feasible years, with the goodness of fit above 0.6 decreased to 25.

The results are summarised in Table A4.7 The estimated effective rainfall nonlinearity has an exponential shape, similar to the Axe catchment. The parameters of second order model a_1, a_2, b_0, b_1 were estimated together with the effective rainfall parameter γ. The first column of the table (period) refers to the middle point of the time horizon of each event. The goodness of fit criterion R_T^2 is given in the last column (see also Figure A4.74). The identified nonlinearities for each period are shown in Figure A4.67

Table A4.7 Parameters of the DBM model for Teme

period	a_1	a_2	b_0	b_1	γ	R_T^2
1986.91	-1.70	0.70	0.02	-0.01	0.05	0.81
1987.34	-1.76	0.76	0.02	-0.02	0.01	0.80
1987.92	-1.97	0.97	0.01	-0.01	0.00	0.88
1988.50	-1.92	0.92	0.01	-0.01	0.00	0.76
1988.95	-1.88	0.88	0.01	-0.01	0.08	0.81
1989.40	-1.83	0.83	0.02	-0.01	0.00	0.85
1990.19	-1.97	0.97	0.01	-0.01	0.01	0.91
1990.92	-1.98	0.98	0.01	-0.01	0.04	0.93
1991.42	-1.96	0.96	0.01	-0.01	0.01	0.84
1991.97	-1.89	0.89	0.02	-0.02	0.04	0.85
1992.52	-1.94	0.94	0.01	-0.01	0.00	0.60
1993.06	-1.97	0.97	0.01	-0.01	0.03	0.91
1993.61	-1.95	0.95	0.01	-0.01	0.02	0.87
1994.16	-1.95	0.95	0.01	-0.01	0.03	0.84
1995.31	-1.98	0.98	0.01	-0.01	0.05	0.91
1996.38	-1.99	0.99	0.01	-0.01	0.05	0.62
1996.97	-1.99	0.99	0.01	-0.01	0.06	0.87
1997.44	-1.96	0.96	0.01	-0.01	0.00	0.92
2000.51	-1.74	0.75	0.02	-0.02	0.02	0.92
2000.96	-1.97	0.97	0.02	-0.02	0.02	0.86
2001.45	-1.93	0.93	0.01	-0.01	0.00	0.68
2001.94	-1.92	0.92	0.02	-0.02	0.01	0.83
2002.43	-1.93	0.93	0.01	-0.01	0.02	0.85
2002.92	-1.98	0.98	0.01	-0.01	0.02	0.90
2003.41	-2.00	1.00	0.00	0.00	0.04	0.79

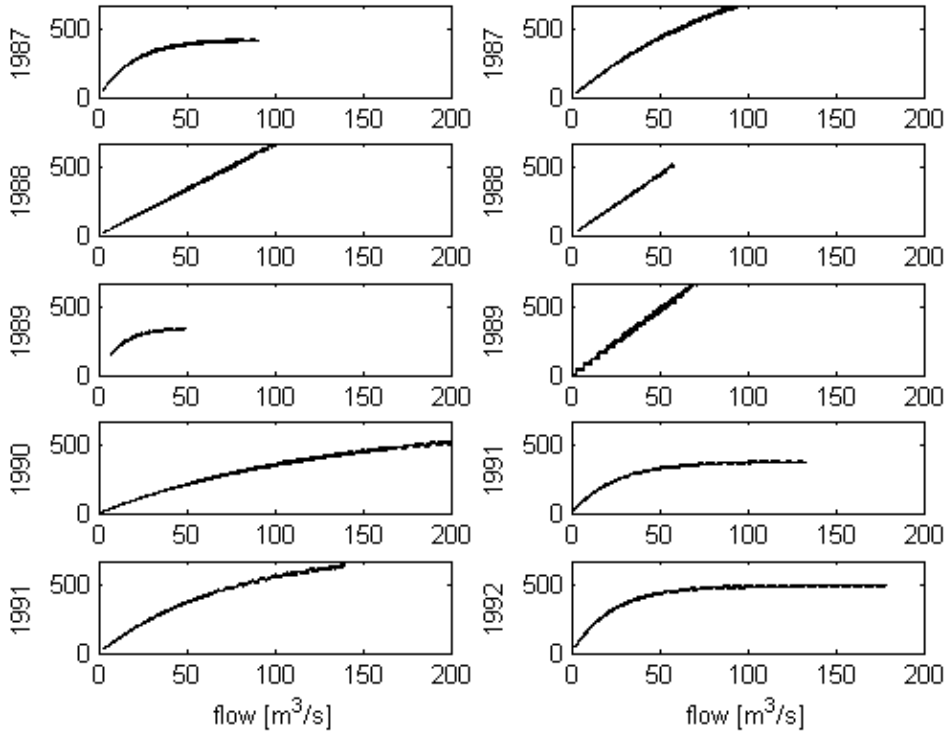

Figure A4.67a Nonlinear gains for the years 1987-1992 with 0.95 confidence bounds

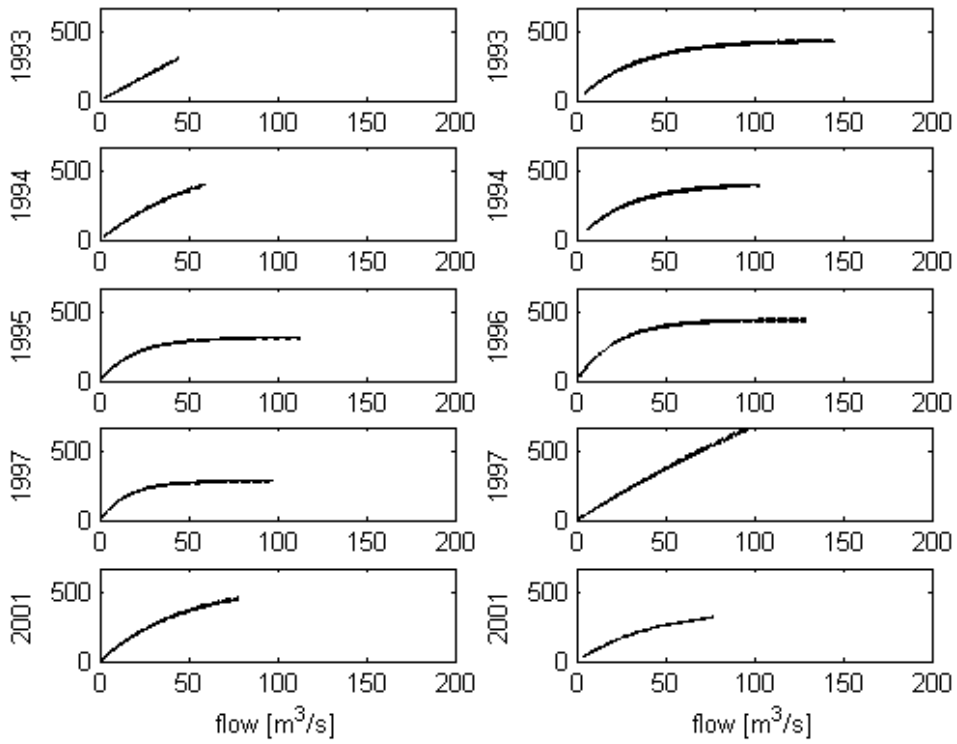

Figure A4.67b Nonlinear gains for the years 1993-2001 with 0.95 confidence bounds

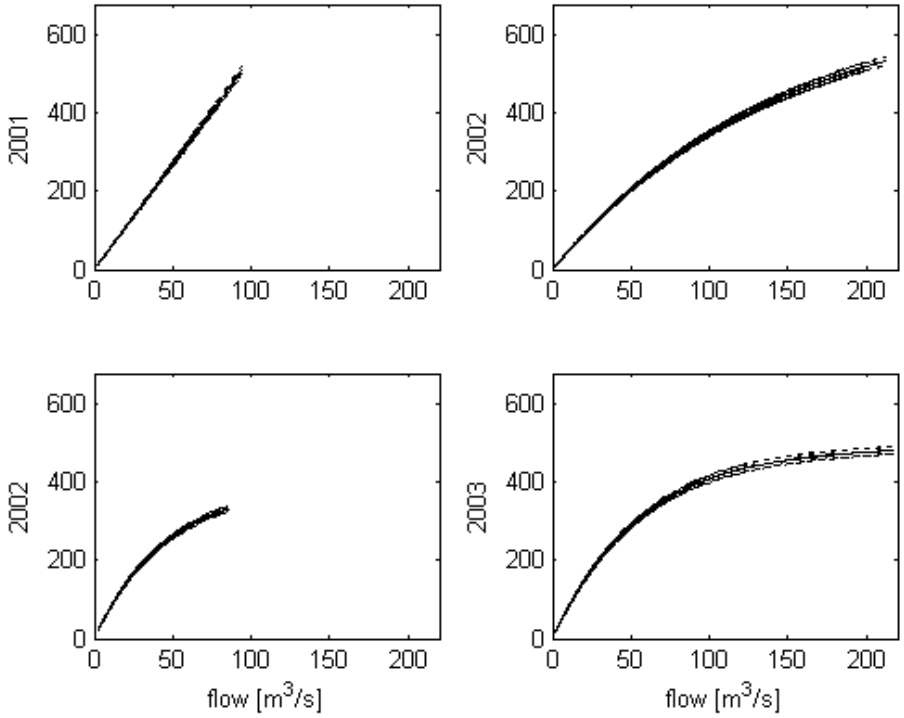

Figure A4.67c Nonlinear gains for the years 2001-2003 with 0.95 confidence bounds

A4.7.4 Analysis of DBM model results for Teme.

There are no clear trends in the derived variables of the DBM models with time or with maximum flow and total rainfall for each period.

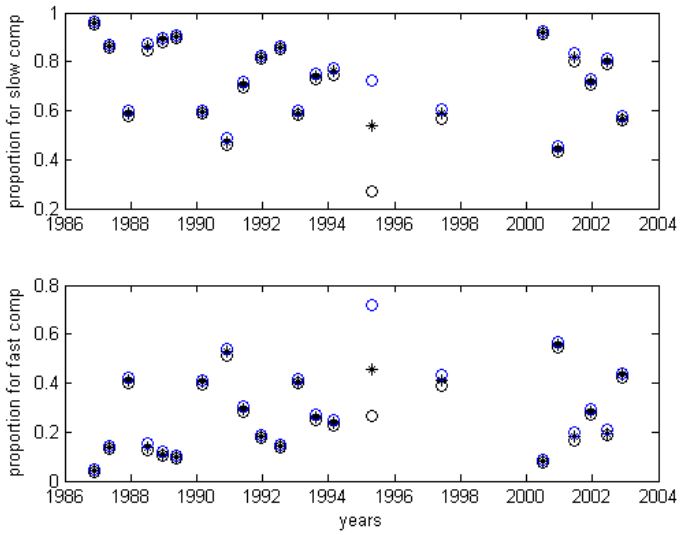

Figure A4.68 Proportions of total discharge with 0.95 confidence bounds identified for slow component (upper panel) and fast flow component (lower panel).

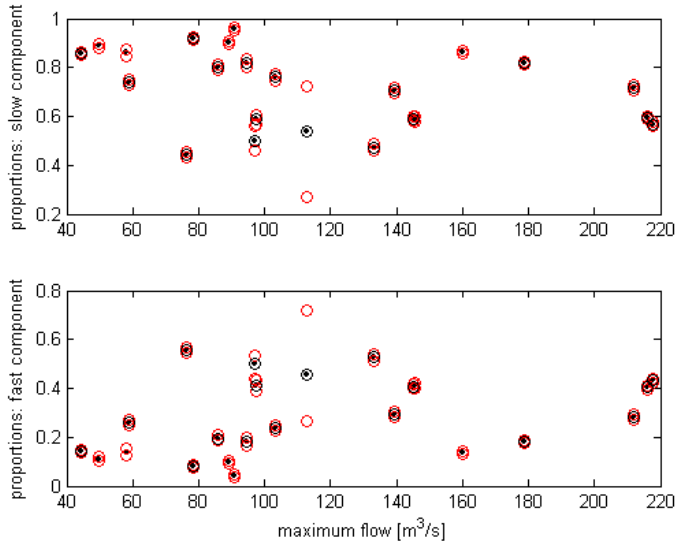

Figure A4.69 proportions as a function of maximum flow (black dots) with 0.95 confidence bounds (red circles). Black circles denote events from the years 1990-2003

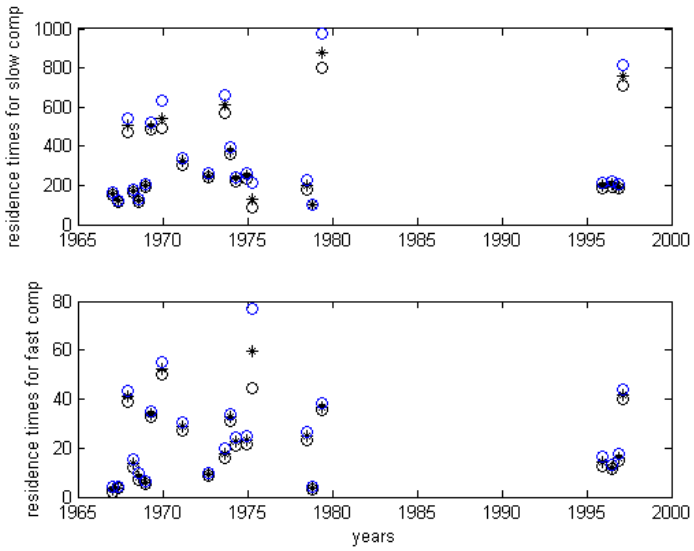

Figure A4.70 Residence times (hours) with 0.95 confidence bounds identified for slow component (upper panel) and fast flow component (lower panel).

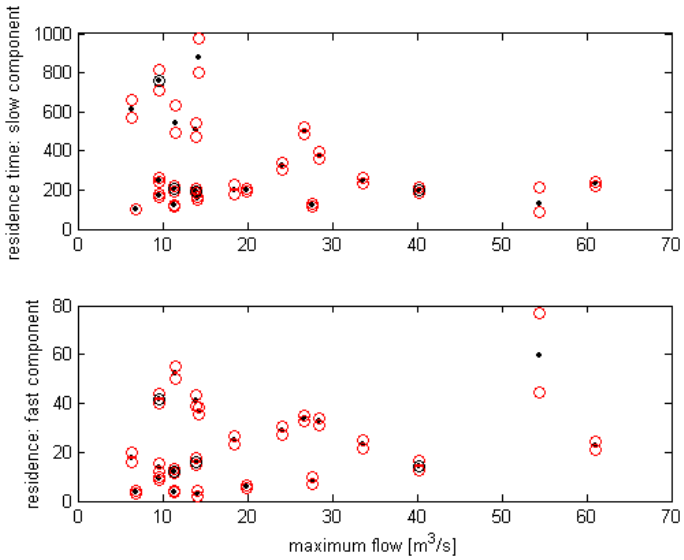

Figure A4.71 Residence times (hours) as a function of maximum flow (black dots) with 0.95 confidence bounds (red circles). Black circles denote events from the years 1990-2003

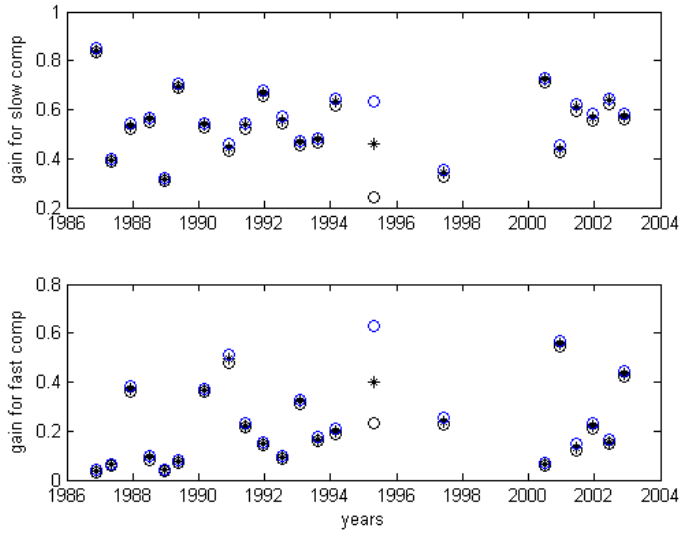

Figure A4.72 Gains with 0.95 confidence bounds identified for slow component (upper panel) and fast flow component (lower panel).

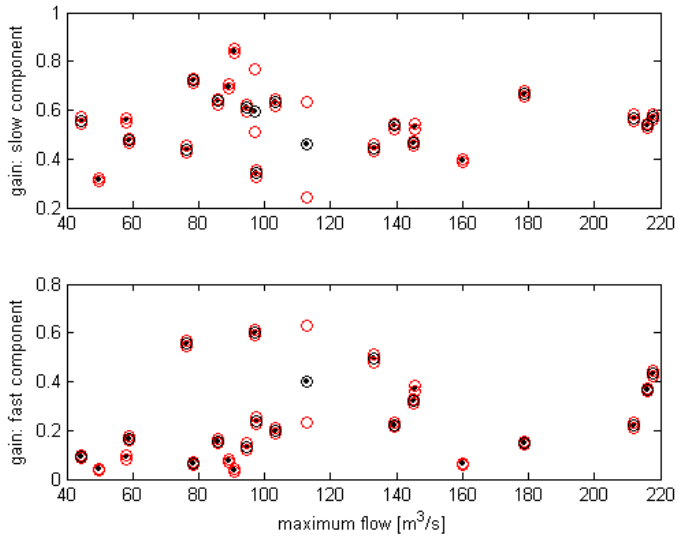

Figure A4.73 Gains as a function of maximum flow (black dots) with 0.95 confidence bounds (red circles). Black circles denote events from the years 1990-2003

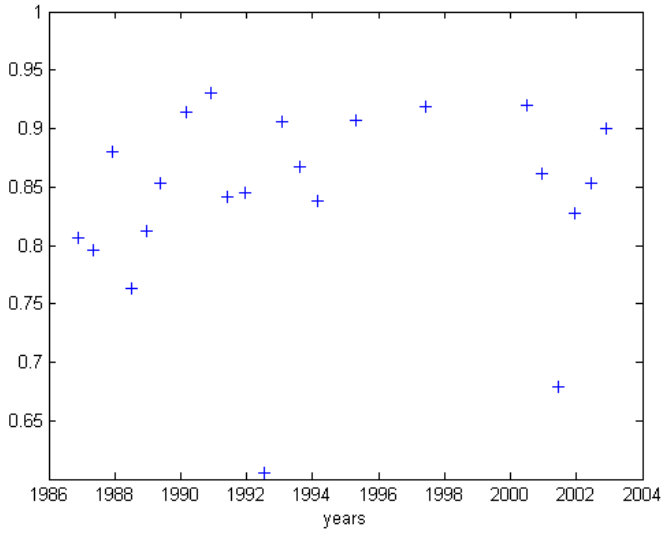

Figure A4.74 Goodness of fit of DBM models

A4.8 Wye

A4.8.1 Catchment data

The Derbyshire Wye flow data are measured at Ashford gauging station. The catchment area is 154 km^2. It is a moderate to high relief catchment in the South Pennines. The geology is primarily Carboniferous Limestone with some basic sills and intrusions in the upper catchment. There are isolated patches of hill top peat and boulder clay. The town of Buxton is situated in the headwaters. Elsewhere there is moorland and improved grazing with some forest in the main valley. Digital flow data start in 1971 and end in 2003 (Figure A4.75). 15 mins rainfall measurements start in 1980 and finish in 2004. There are also daily measurements available, which we use for the DHR analysis, as these sets are usually longer and more reliable. The rainfall and flow data correspond to each other well, as indicated by good model fits (Figure A4.85).

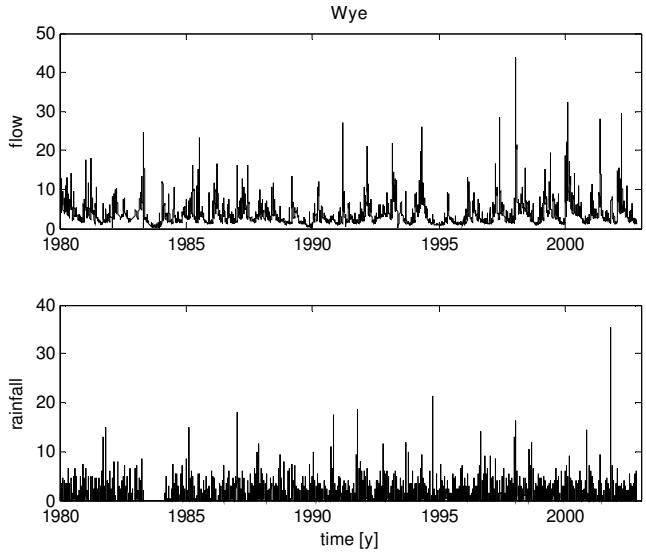

Figure A4.75 Rainfall and flow for Wye

A4.8.2 DHR analysis

DHR analysis is performed on monthly data. We use smoothed monthly data for flow and monthly cumulative rainfall data obtained from daily measurements. The rainfall gauging station is situated at the catchment outflow, near the water level gauging station. Figure A4.76 presents the comparison of trends obtained for the logarithm of flow (upper panel) and rainfall (lower panel). Figure A4.77 is the illustration of the nonstationary monthly trends in the catchment. There is no statistical evidence of the change in trend neither for the flow nor for the rain for this catchment.

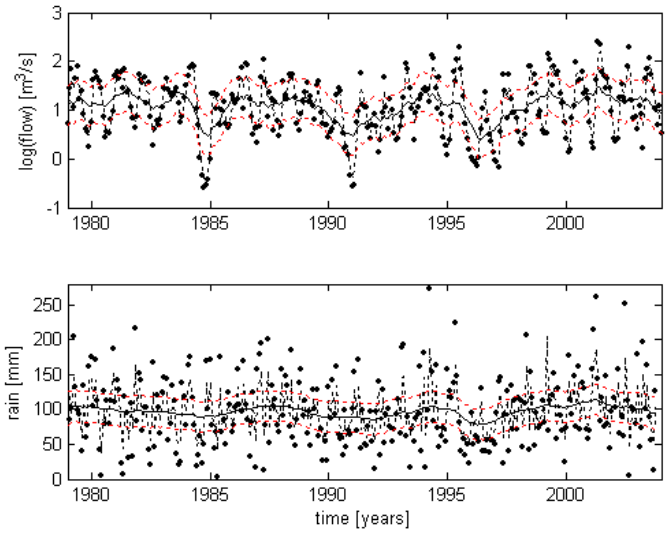

Figure A4.76. Comparison of trends for flow (upper panel) and rainfall (lower panel)

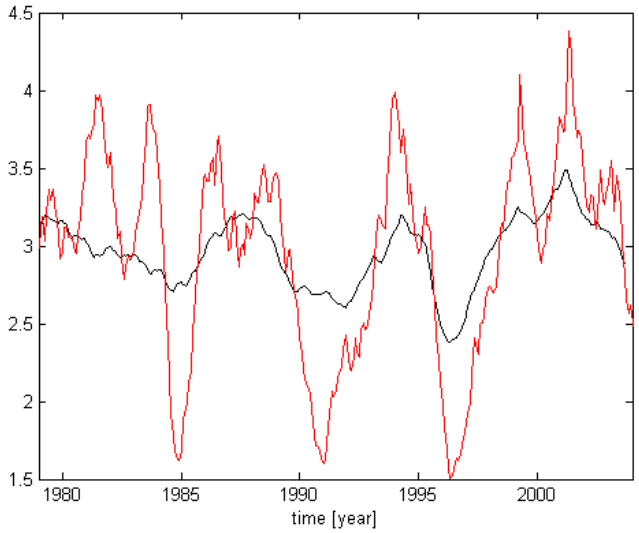

Figure A4.77 Nonstationary trends in monthly rainfall and flows in the Wye catchment scaled to equal total volumes, red line shows the trend of the flow and black line presents the rainfall trend.

A4.8.3 DBM analysis

The typical best linear catchment model has second order structure [2 2 0].

The results of the DBM analysis are summarised in Table A8. The estimated effective rainfall nonlinearity has an exponential shape, similar to the Axe catchment. The parameters of second order model a_1, a_2, b_0, b_1 were estimated together with the

effective rainfall parameter γ. The first column of the table (period) refers to the middle point of the time horizon of each event. The goodness of fit criterion R_T^2 is given in the last column.

Table A.8. Parameters of the DBM models for Wye

period	a_1	a_2	b_0	b_1	γ	R_T^2
1981.877	-1.952	0.952	0.007	-0.007	0.022	0.918
1988.823	-1.946	0.946	0.004	-0.004	0.000	0.892
1989.985	-1.981	0.981	0.006	-0.006	0.000	0.801
1990.985	-1.984	0.984	0.007	-0.007	0.014	0.899
1993.988	-1.968	0.968	0.008	-0.008	0.030	0.941
1994.988	-1.970	0.970	0.007	-0.007	0.000	0.917
1996.988	-1.988	0.988	0.005	-0.005	0.069	0.888
1998.128	-1.970	0.970	0.008	-0.008	0.112	0.936
1998.945	-1.966	0.966	0.012	-0.011	0.037	0.895
1999.945	-1.926	0.926	0.010	-0.009	0.054	0.922
2000.945	-1.974	0.974	0.010	-0.010	0.161	0.943
2001.948	-1.988	0.988	0.004	-0.004	0.000	0.888

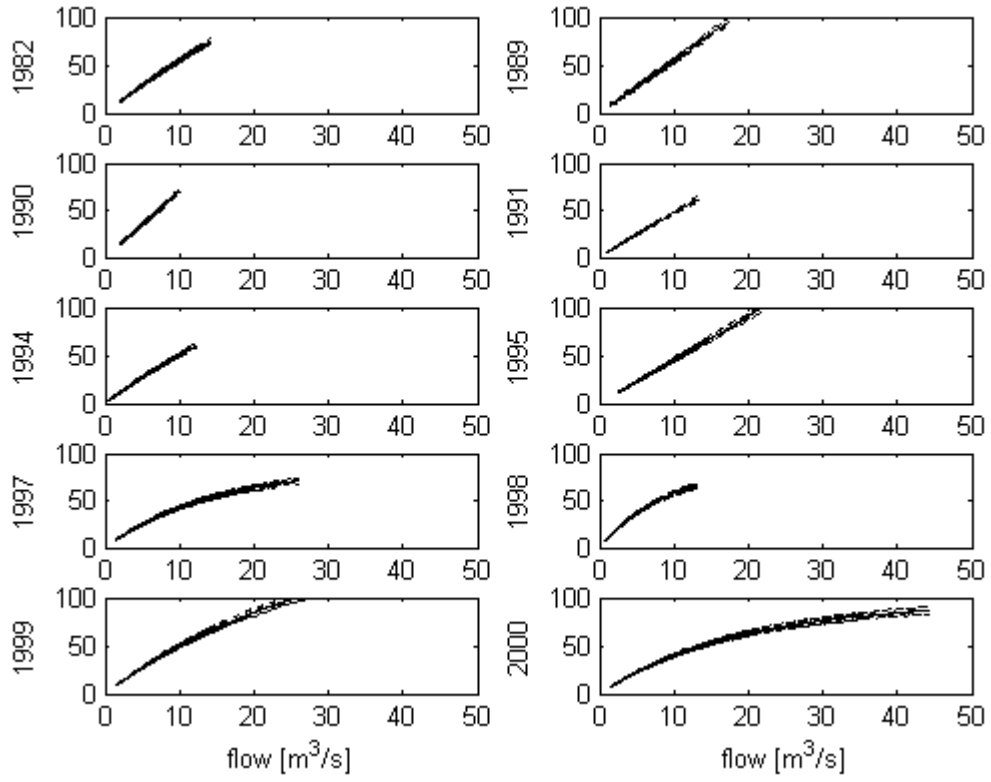

Figure A4.78a. Nonlinear gain for the years 1982-2000.

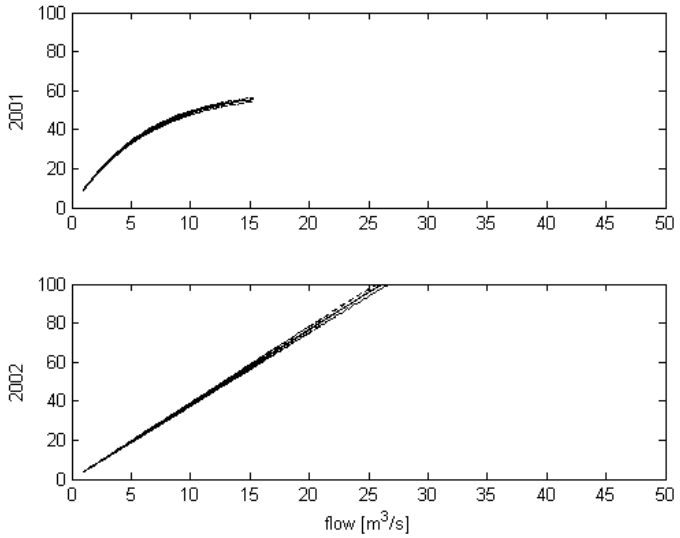

Figure A4.78b. Nonlinear gain for the years 2001-2002.

Figure A4.78a,b presents the nonlinear gain used for each of the years within the feasible periods.

A4.8.4 Analysis of DBM model results

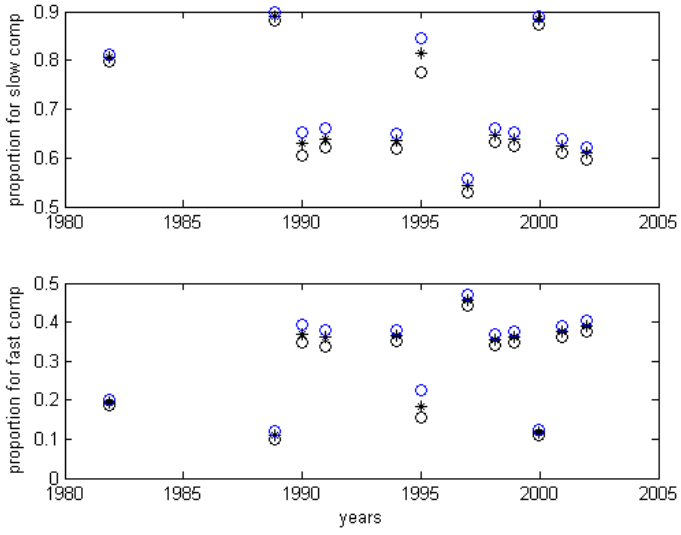

Figure A4.79 Estimates of partition for the slow (upper panel) and fast (lower panel) flow components for different years; stars denote estimates of gain with uncertainty of the model and effective rainfall transformation parameters taken into account; circles denote the lower and upper 0.95 confidence bounds.

Figure A4.79 presents the estimates of slow (upper panel) and fast (lower panel) component partitioning together with 0.95 confidence bands. Figure A4.80 presents the proportions as a function of maximum flow. Figure A4.81 presents the residence times as a function of time and Figure A4.82 shows the residence times against maximum flow.

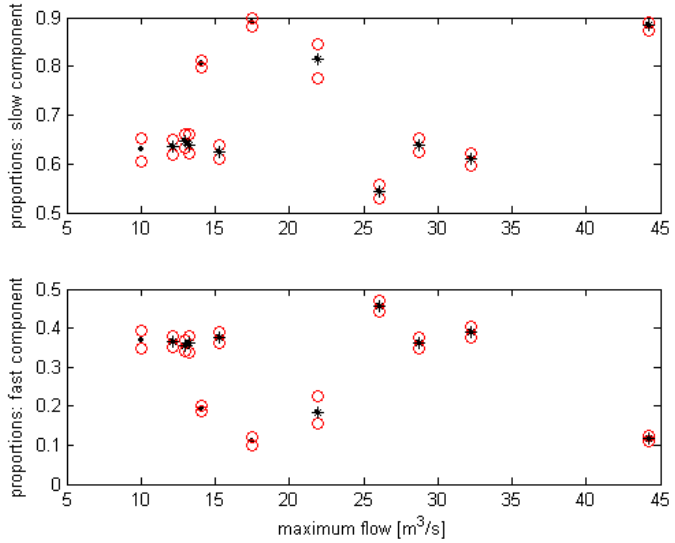

Figure A4.80 Proportions as a function of maximum flow (black dots) with 0.95 confidence bounds (red circles) against maximum flow. Black circles denote events from the years 1980-2004

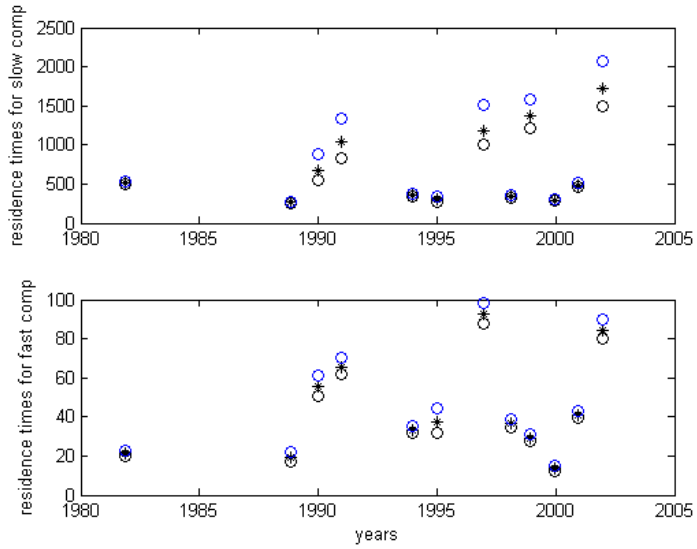

Figure A4.81 Estimates of residence times (hours) for the slow (upper panel) and fast (lower panel) flow components for different years; stars denote estimates of residence time with uncertainty of model and effective rainfall transformation parameters taken into account; circles denote the lower and upper 0.95 confidence bounds.

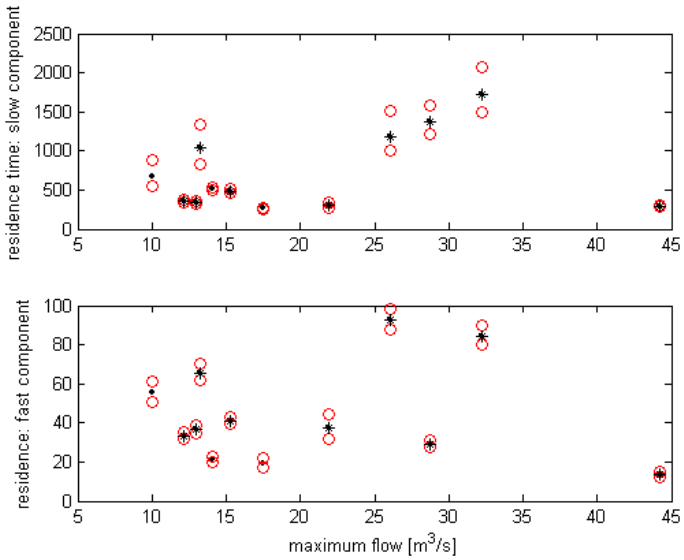

Figure A4.82 Residence times (hours) as a function of maximum flow (black dots) with 0.95 confidence bounds (red circles). Black circles denote events from the years 1980-2004

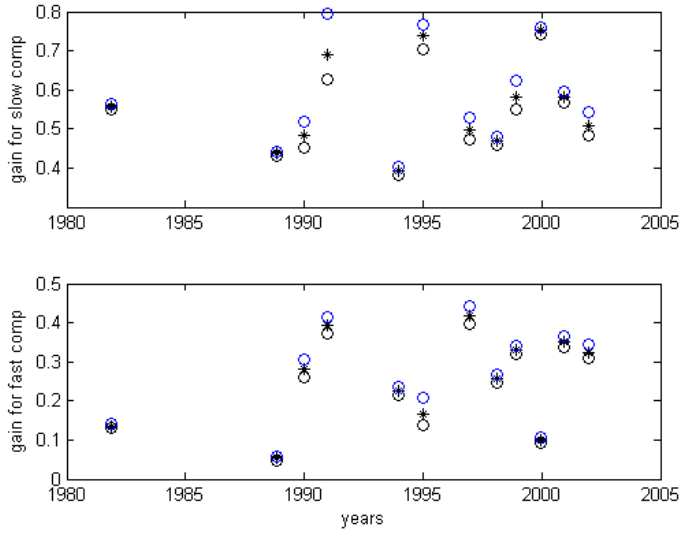

Figure A4.83. Estimates of gains for the slow (upper panel) and fast (lower panel) flow components for different years; stars denote estimates of gain with uncertainty of the model and effective rainfall transformation parameters taken into account; circles denote the lower and upper 0.95 confidence bounds.

Figures A4.83 and A4.84 present gains estimates as a function of time and maximum flow respectively.

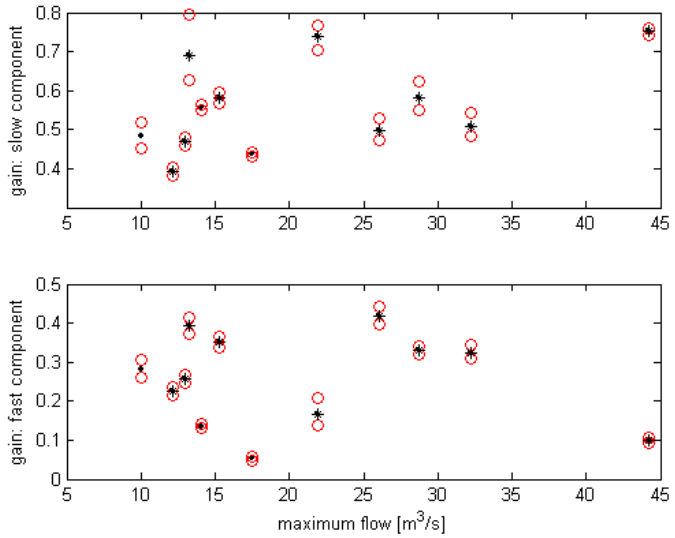

Figure A4.84 Gains as a function of maximum flow (black dots) with 0.95 confidence bounds (red circles). Black circles denote events from the years 1980-2004

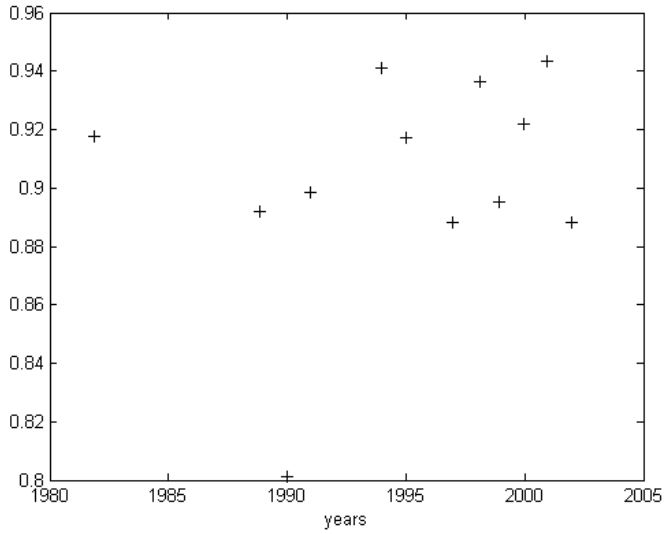

Figure A4.85 Goodness of fit of DBM models

Figure A4.85 shows the goodness of fit for the models developed for the Wye.

Ergon House
Horseferry Road
London SW1P 2AL

www.defra.gov.uk